ORIGINAL ARTICLE

A Novel CD4$^+$ T Cell–Dependent Murine Model of *Pneumocystis*-driven Asthma-like Pathology

Taylor Eddens[1,2], Brian T. Campfield[1,3], Katelin Serody[1], Michelle L. Manni[4], William Horne[1], Waleed Elsegeiny[1,2], Kevin J. McHugh[4], Derek Pociask[5], Kong Chen[1], Mingquan Zheng[1], John F. Alcorn[4], Sally Wenzel[6], and Jay K. Kolls[1]

[1]Richard King Mellon Foundation Institute for Pediatric Research and [4]Department of Pediatrics, Children's Hospital of Pittsburgh of UPMC, Pittsburgh, Pennsylvania; [2]Department of Immunology, [3]Division of Pediatric Infectious Diseases, Department of Pediatrics, and [6]Division of Pulmonary, Allergy, and Critical Care Medicine, University of Pittsburgh School of Medicine, Pittsburgh, Pennsylvania; and [5]Department of Pulmonary Diseases, Critical Care, and Environmental Medicine, Tulane University School of Medicine, New Orleans, Louisiana

Abstract

Rationale: Infection with *Pneumocystis*, an opportunistic fungal pathogen, can result in fulminant pneumonia in the clinical setting of patients with immunosuppression. In murine models, *Pneumocystis* has previously been shown to induce a CD4$^+$ T cell–dependent eosinophilic response in the lung capable of providing protection.

Objectives: We sought to explore the role of *Pneumocystis* in generating asthma-like lung pathology, given the natural eosinophilic response to infection.

Methods: *Pneumocystis* infection or antigen treatment was used to induce asthma-like pathology in wild-type mice. The roles of CD4$^+$ T cells and eosinophils were examined using antibody depletion and knockout mice, respectively. The presence of anti-*Pneumocystis* antibodies in human serum samples was detected by ELISA and Western blotting.

Measurements and Main Results: *Pneumocystis* infection generates a strong type II response in the lung that requires CD4$^+$ T cells. *Pneumocystis* infection was capable of priming a Th2 response similar to that of a commonly studied airway allergen, the house dust mite. *Pneumocystis* antigen treatment was also capable of inducing allergic inflammation in the lung, resulting in anti-*Pneumocystis* IgE production, goblet cell hyperplasia, and increased airway resistance. In the human population, patients with severe asthma had increased levels of anti-*Pneumocystis* IgG and IgE compared with healthy control subjects. Patients with severe asthma with elevated anti-*Pneumocystis* IgG levels had worsened symptom scores and lung parameters such as decreased forced expiratory volume and increased residual volume compared with patients with severe asthma who had low anti-*Pneumocystis* IgG.

Conclusions: The present study demonstrates for the first time, to our knowledge, that *Pneumocystis* is an airway allergen capable of inducing asthma-like lung pathology.

Keywords: allergic inflammation; asthma; *Pneumocystis*; T cells

At a Glance Commentary

Scientific Knowledge on the Subject: The present study demonstrates that *Pneumocystis* infection can cause Th2-driven lung pathology phenocopying that of other common airway allergens. It identifies *Pneumocystis* as a novel aeroallergen capable of mediating allergic inflammation.

What This Study Adds to the Field: The present study establishes a novel relationship between *Pneumocystis* and asthma in both murine and human models.

(Received in original form November 12, 2015; accepted in final form March 15, 2016)

Supported by National Institute of Allergy and Infectious Diseases grants F30 AI114146 (T.E.) and P01AI106684 (S.W. and J.K.K.), NHLBI grants R01 HL062052 (J.K.K.), K08HL128809 (B.T.C.), and R01 HL107380 (J.F.A.), an American Heart Association postdoctoral fellowship (M.L.M.), and NHLBI grant R01 HL69174 under the Severe Asthma Research Program (S.W.).

Author Contributions: T.E. was responsible for the majority of the experimental design, acquired and analyzed data, and wrote the manuscript; B.T.C. and K.S. contributed to the experimental design, the acquisition and analysis of data, and the writing of the manuscript; M.L.M., W.H., W.E., K.J.M., D.P., K.C., and M.Z. provided technical assistance in flexiVent studies, RNA sequencing, flow cytometry, and pathologic scoring; J.F.A. provided mentorship and guidance in assessment of lung function; S.W. provided mentorship and human samples; and J.K.K. was the primary mentor on the project.

Correspondence and requests for reprints should be addressed to Jay K. Kolls, M.D., Richard King Mellon Foundation Institute for Pediatric Research, Children's Hospital of Pittsburgh of UPMC, Rangos Research Building, 4401 Penn Avenue, Pittsburgh, PA 15224. E-mail: jay.kolls@chp.edu

This article has an online supplement, which is accessible from this issue's table of contents at www.atsjournals.org

Am J Respir Crit Care Med Vol 194, Iss 7, pp 807–820, Oct 1, 2016
Copyright © 2016 by the American Thoracic Society
Originally Published in Press as DOI: 10.1164/rccm.201511-2205OC on March 23, 2016
Internet address: www.atsjournals.org

Asthma affects over 300 million people worldwide and up to 30% of children in Western countries (1, 2). Although asthma has more recently become recognized as a heterogeneous disorder, asthma in childhood is classically characterized by activation of type II immune responses (3–6). Type II cells—for example, Th2 and type II innate lymphoid (ILC2) cells—can release IL-4 as well IL-5 and IL-13 in the lung, resulting in eosinophilic inflammation, goblet cell hyperplasia, and bronchial hyperreactivity (7, 8).

Although asthma is a genetically heterogeneous disease, recent genome-wide association studies have associated certain genes, such as *IL33*, *SMAD3*, and *HLA-DQ*, with the presence of asthma in all age groups (9). In addition to genetic factors, however, it is clear that early-life exposure to pathogens such as respiratory syncytial virus can contribute to the development of asthma (10, 11). A variety of other airborne exposures can exacerbate asthma, such as house dust mite (HDM), cigarette smoke, and fungal species (12). Interestingly, patients with fungal IgE sensitization have more severe asthma as measured by diminished lung function and increased hospital admissions (13–15). Importantly, numerous animal models have demonstrated that fungal sensitization can increase airway hyperresponsiveness and contribute to asthma-like pathology (16, 17).

Pneumocystis jirovecii is an opportunistic fungal pathogen that causes diffuse interstitial pneumonia in both HIV-positive and HIV-negative immunosuppressed populations (18–20). *Pneumocystis* (PC) exposure occurs early in the first year of life, typically causing fulminant pneumonia in infants with immunodeficiency (19, 21). In one study of postmortem infant lung tissues, researchers found that the majority of infants, regardless of immune status, had detectable PC RNA in their lungs by the age of 4 months (21). However, PC exposure persists throughout all stages of life, as PC nucleic acids have been found in the lungs of healthy adults and in individuals with chronic lung diseases (22–24). These studies demonstrated that PC can persist asymptomatically in the lung at low levels (colonization) and that person-to-person transmission may result in frequent exposure in the general population (25). In support of this notion, one study showed that 52% of children had anti-PC antibodies by the age of 6 years and that this percentage rose to 80% by the age of 13 years (26).

The HIV/AIDS epidemic in the 1980s clearly implicated $CD4^+$ T cells as primary mediators of immunity to PC, which was later confirmed in murine models (27, 28). Once primed, $CD4^+$ T cells generate type II responses and facilitate production of protective anti-PC antibodies (29, 30). One early effector function of $CD4^+$ T cells is to recruit eosinophils to the lungs, which subsequently reduces PC burden (31). Given the strong eosinophilic response to PC in the lung and the abundance of exposure to PC among the general population, we hypothesized that PC may generate a type II response capable of modulating a similarly type II–driven disease of the lung, asthma.

Methods

Mice

C57BL/6, BALB/c, *Gata1*^{tm6Sho}*/J*, *Rag1*$^{-/-}$, and *Rag2*$^{-/-}$*Il2rg*$^{-/-}$ mice were all ordered from The Jackson Laboratory (Bar Harbor, ME). All of the mice were 6–8 weeks old and sex matched. Colonies were maintained in the Rangos Research Building Animal Facility, and their use in experiments was carried out with approval by and in accordance with the policies of the University of Pittsburgh Institutional Animal Care and Use Committee.

Pneumocystis Inoculation

Pneumocystis murina was harvested from the lungs of an infected *Rag2*$^{-/-}$*Il2rg*$^{-/-}$ mouse, and mice were challenged with 2.0×10^6 cysts per milliliter as previously described (32, 33). CD4 depletion with GK1.5 antibody was performed as described previously (28, 32).

RNA Isolation and Quantitative Reverse Transcriptase–Polymerase Chain Reaction

The right middle lobe was homogenized in TRIzol reagent (Life Technologies, Carlsbad, CA) and then subjected to RNA isolation per the manufacturer's instructions. RNA (1 μg) was then converted to cDNA using an iScript kit (Bio-Rad Laboratories, Hercules, CA). Gene expression analysis was performed using quantitative reverse transcriptase–polymerase chain reactions with SsoAdvanced Universal Probes Supermix (Bio-Rad Laboratories). Murine primers used included *Il4*, *Il5*, *Il13*, *Clca3*, *Muc5ac*, and *Prg2* (Applied Biosystems, Foster City, CA). The PC small subunit primer and probe sequences used were as follows: forward: 5′-CATTCCGAGAACGAACGCAATCCT; reverse: 5′-TCGGACTTGGATCTTT GCTTCCCA; and 6-carboxyfluorescein probe: 5′-TCATGACCCTTATG GAGTGGGCTACA.

RNA Sequencing

Sample preparation and RNA sequencing were performed as described previously (31); this information is publicly available through the Sequence Read Archive BioProject (number PRJNA276259). Data were filtered on a quality score of 10 and mined for the following genes associated with type II immune responses: *Il33*, *Il25*, *Muc5ac*, *Clca3*, *Il9*, *Il4*, *Il13*, *Chi3l3*, *Chi3l4*, *Arg1*, *Il9r*, *Il17rb*, *Gpr44*, *Tslp*, *Il7r*, *Crlf2*, *Il1rl1*, and *Acta2*. *Il9* and *Il25* did not pass the quality filter.

Lung Protein and Luminex Assay

The right upper lobe of the lung was collected and then homogenized in phosphate-buffered saline (PBS) plus protease inhibitor (14277300; Roche, Indianapolis, IN). The lung homogenate was then centrifuged at $5{,}000 \times g$ for 5 minutes for debris removal, and the supernatant was collected. Cytokine analysis was then performed on this supernatant with a 23-plex Bio-Plex Pro assay (Bio-Rad Laboratories) per the manufacturer's instructions.

Ex Vivo Whole-Lung Cell Stimulation

The right lower and postcaval lobes of the lung were collected, physically digested, and incubated for 1.5 hours at 37°C in collagenase/DNase. Lungs were collected from naive, HDM-treated, PC-infected, or HDM-treated and PC-infected mice. Likewise, cells were isolated from mice treated with *Pneumocystis* antigen (PCAg). Single-cell suspensions were then strained using a 70-μm sterile filter, treated with red blood cell lysis buffer (NH_4Cl), and enumerated. A total of 5×10^5 cells per well were stimulated with PBS (no-stimulation control), 2.5 μg of PCAg or HDM, or 2.5 μl of CD3/CD28 Dynabeads (2015-07; Life Technologies). Three days

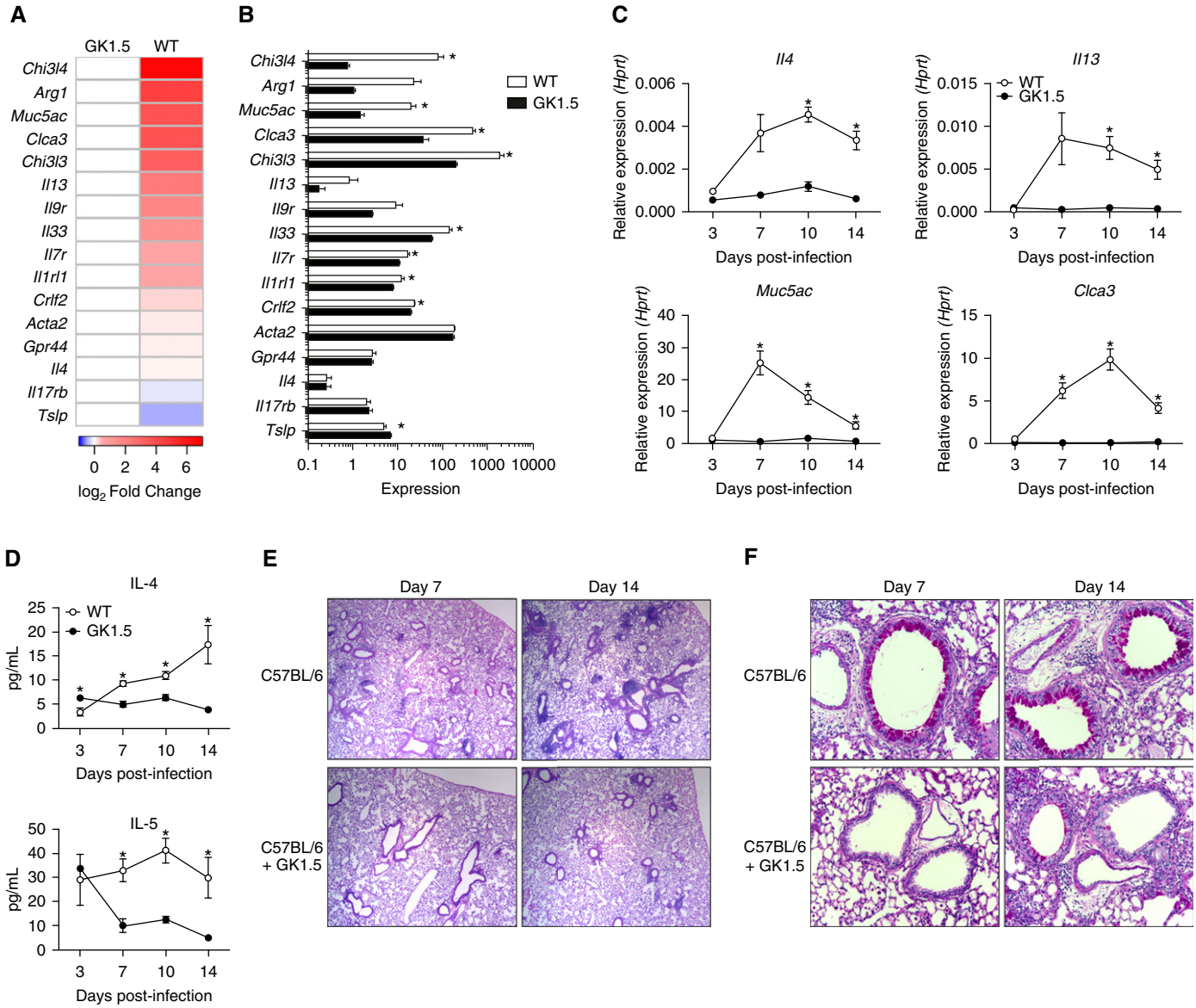

Figure 1. *Pneumocystis murina* infection induces a CD4$^+$ T cell–dependent type II response. Wild-type (WT) or GK1.5-treated C57BL/6 mice were infected with *P. murina* and killed at Day 3, 7, 10, or 14. (*A*) Whole-lung RNA from Day 14 was then isolated, sequenced using an Illumina NextSeq 500 sequencer (Illumina, San Diego, CA), and analyzed for differential expression of genes associated with a type II response. (*B*) Heat map showing RNA sequencing expression levels for the corresponding genes (*$P < 0.05$ by Student's *t* test; n = 4 per group). (*C*) Expression of *Il4*, *Il13*, *Muc5ac*, and *Clca3* over the time course, as measured by quantitative reverse transcriptase–polymerase chain reaction, demonstrating CD4$^+$ T cell–dependent increases in gene expression (*$P < 0.05$ by two-way analysis of variance with multiple comparisons; n = 5). (*D*) Protein levels of IL-4 and IL-5 in WT and GK1.5-treated mice during infection. (*E*) Representative hematoxylin and eosin staining of sectioned lung from WT and GK1.5-treated mice at Days 7 and 14 demonstrating increased eosinophilic perivascular inflammation in WT mice. (*F*) Representative periodic acid–Schiff staining of sectioned lung from WT and GK1.5-treated mice at Days 7 and 14 demonstrating increased mucus production in WT animals. *Hprt* = hypoxanthine phosphoribosyltransferase.

post-stimulation, the cells were pelleted, supernatants were harvested, and cell pellets were resuspended in TRIzol LS reagent (Life Technologies).

Histology

The right lung was clamped, and the left lung was inflated with 10% formalin through the trachea. Following fixation, the lungs were processed, sectioned, and stained with hematoxylin and eosin or periodic acid–Schiff (PAS).

Pneumocystis Antigen Preparation and Treatment

A lung from a *Rag2*$^{-/-}$*Il2rg*$^{-/-}$ mouse infected with *P. murina* for 8 weeks was strained through a 70-μm sterile filter (29, 32). Following centrifugation, the pellet was resuspended in 1 ml of PBS, layered on top of 30 ml of Centricoll (C-0580; Sigma-Aldrich, St. Louis, MO), and centrifuged at 2,000 rpm for 15 minutes. The material at the interface of the Centricoll and PBS was collected, washed twice in PBS, resuspended in 1 ml of PBS, and sonicated for 30 seconds three times. Protein was

quantified using a bicinchoninic acid assay. Mice were then anesthetized with isoflurane, and 10 μg of PCAg or HDM was administered intranasally in 50 μl of PBS. Mice were sensitized on Day 0, challenged on Days 7–11, and killed on Day 14. For ILC2 studies, mice were treated every 3 days intraperitoneally with 0.5 mg of anti-ST2 antibody, provided by Dr. Dirk Smith.

ELISAs and Western Blotting

Additional details on the methods for making these measurements is provided in the online supplement.

Lung Mechanics and Airway Hyperresponsiveness Measurements

Pulmonary function was assessed during mechanical ventilation of anesthetized (90 mg/kg pentobarbital intraperitoneally) and tracheotomized mice using a computer-controlled small-animal mechanical ventilator (flexiVent; SCIREQ, Montreal, QC, Canada) as previously described (34, 35). Quasistatic compliance, Newtonian resistance, tissue damping, and tissue elastance were calculated as described previously (36, 37). Further information can be found in the online supplement.

Clinical Measurements

All human samples were collected via the Severe Asthma Research Program and were collected at the University of Pittsburgh. Samples were deidentified, and serum ELISAs were performed by a researcher blinded to disease status. Symptom scores and clinical measurements were collected in accordance with the institutional review board's approval (IRB0610032) as previously described (4).

Statistics

All statistics were performed using Prism version 6.0f software (GraphPad Software, La Jolla, CA). All data are presented with mean ± SEM. For studies with two groups, we used a simple Student's *t* test. Time-course and flexiVent studies were analyzed using two-way analysis of variance (ANOVA) with multiple comparisons at each time point. Studies with more than two samples were analyzed using ordinary one-way ANOVA with Tukey's multiple comparisons. Cytokine protein levels were analyzed for normality using a D'Agostino and Pearson omnibus normality test and were found to be normally distributed. Antibody dilution studies with human serum were analyzed using two-way ANOVA. A χ^2 test was used to analyze patient symptom scores. Linear regression was performed; the slope was analyzed for significant difference from zero; and Pearson's correlation coefficient was calculated. In all statistical analyses, we considered $P < 0.05$ significant.

Results

P. murina Infection Induces a Robust Type II Response Dependent on $CD4^+$ T Cells

We previously showed that *P. murina* infection leads to a $CD4^+$ T cell–dependent recruitment of eosinophils (31). In the present study, however, we found by RNA sequencing that several other genes associated with a type II response were upregulated in wild-type mice compared with CD4-depleted mice treated with GK1.5 monoclonal antibody at Day 14 postinfection (Figures 1A and 1B). Moreover, our global pathway analysis demonstrated upregulation of KEGG pathways associated with immunologic function, as well as pathways associated with allergic rhinitis, eosinophilic disorders, and asthma (*see* Figure E1 in the online supplement). In addition to a previously shown increase in IL-5 expression (31), IL-4 and IL-13 were upregulated in a $CD4^+$ T cell–dependent manner (Figure 1C). Likewise, markers of goblet cell hyperplasia, *Muc5ac* and *Clca3*, had increased expression (Figure 1C). At the protein level, IL-4 production over the course of infection increased in a $CD4^+$-dependent manner, while IL-5 had sustained protein levels in wild-type but not $CD4^+$-depleted animals (Figure 1D). Histologically, wild-type mice had inflammatory foci at Day 7 and eosinophilic perivascular inflammation at Day 14, while $CD4^+$-depleted animals appeared to have a delayed and reduced inflammatory response (Figure 1E). Similarly, by Days 7 and 14 of infection, wild-type mice had increased goblet cell activation and mucus production, while GK1.5-treated mice had minimal mucus detected at Day 14 (Figure 1F).

$CD4^+$ T cells are also sufficient to produce a type II immune response following PC infection, as significant increases in *Muc5ac*, *Clca3*, *Il13*, and *Prg2* (major basic protein, an eosinophil marker) were observed in lung homogenates of $Rag1^{-/-}$ mice receiving adoptive transfer of $CD4^+$ T cells compared with no-transfer controls (*see* Figure E2 in the online supplement).

The Immune Response to *Pneumocystis* Generates Type II–mediated Lung Pathology Similar to That of House Dust Mite

We next sought to determine if concurrent PC infection and exposure to a common airway allergen, HDM, would lead to a synergistic type II response (Figure 2A), as prior studies suggested that PC infection altered the immune response to ovalbumin (38). Mice exposed to PC infection or HDM alone generated both anti-PC and anti-HDM IgG and IgE responses in the serum, respectively, while mice subjected to dual treatment generated IgG and IgE to both antigens (Figure 2B). Interestingly, even though all mice exposed to PC infection had cleared the infection by Day 28 (data not shown), mice infected with PC alone had increases in eosinophil and goblet cell hyperplasia transcripts (Figure 2C). A synergistic response was noted in terms of a specific eosinophil marker, *Prg2* (Figure 2C). The antigen-specific responses of whole-lung cells from PC-infected or HDM-exposed mice to PCAg or HDM, respectively, were strikingly similar in terms of IL-4, IL-5, IL-10, IL-13, IL-17A, and IFN-γ production (Figure 2D). Dual treatment resulted in little additive effect and appeared to prime two independent immune responses (Figure 2D). Surprisingly, mice that had been infected with and cleared PC still had detectable mucus in both large and small airways (Figure 2E).

Given the similarities between the antigen-specific responses to primary PC infection and HDM treatment, we next evaluated the potential of PCAg to induce a type II response and lung pathology (Figure 3A). Following sensitization and challenge, mice generated anti-HDM and anti-PC IgG and IgE (Figure 3B). PCAg treatment did increase expression of type II cytokines, mucus-associated genes, and *Prg2* in a manner comparable to that of HDM treatment (Figure 3C). The antigen-specific responses to HDM were similar to those described above

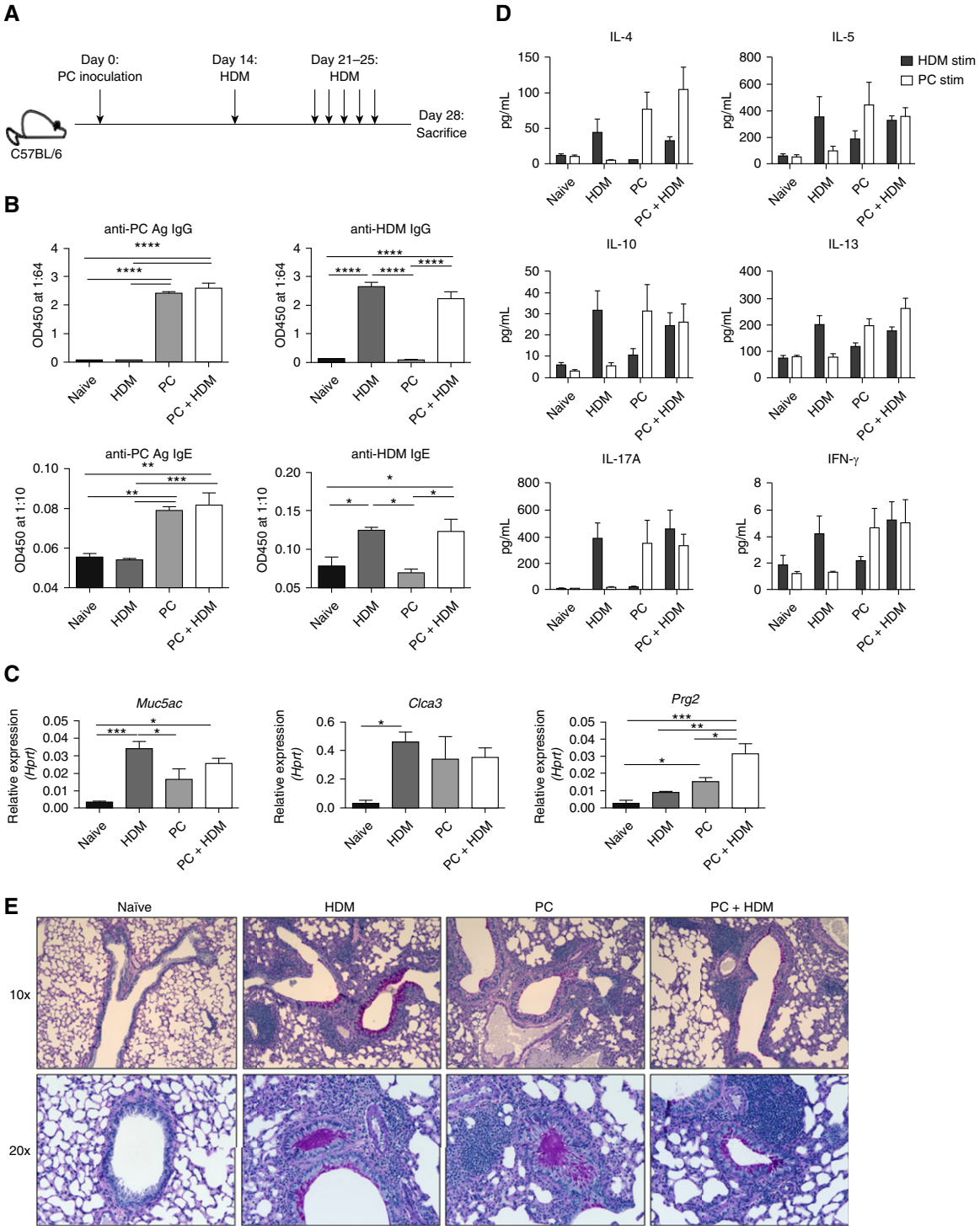

Figure 2. *Pneumocystis* (PC) infection and house dust mite (HDM) treatment induce independent type II responses. (*A*) Mice were untreated (naive), treated with HDM alone, infected with PC alone, or infected with PC and subsequently treated with HDM (n = 4 per group). (*B*) Infection and HDM treatment generated anti-PC and anti-HDM IgG and IgE antibodies. (*C*) Increases in type II–associated genes in PC-infected, HDM-treated, and PC- + HDM-treated mice in whole lung as measured by quantitative reverse transcriptase–polymerase chain reaction. (*D*) *Ex vivo* cells isolated from whole lung were stimulated with either HDM or PC antigen for 72 hours, and supernatants were analyzed using a Bio-Plex kit. (*E*) Periodic acid–Schiff staining of naive, HDM-alone, PC-alone mice, as well as mice that received dual treatment, demonstrating increased mucus production following each treatment (*$P < 0.05$, **$P < 0.01$, ***$P < 0.001$, and ****$P < 0.0001$ by one-way analysis of variance with Tukey's multiple comparisons). Ag = antigen; *Hprt* = hypoxanthine phosphoribosyltransferase; OD450 = optical density at 450 nm.

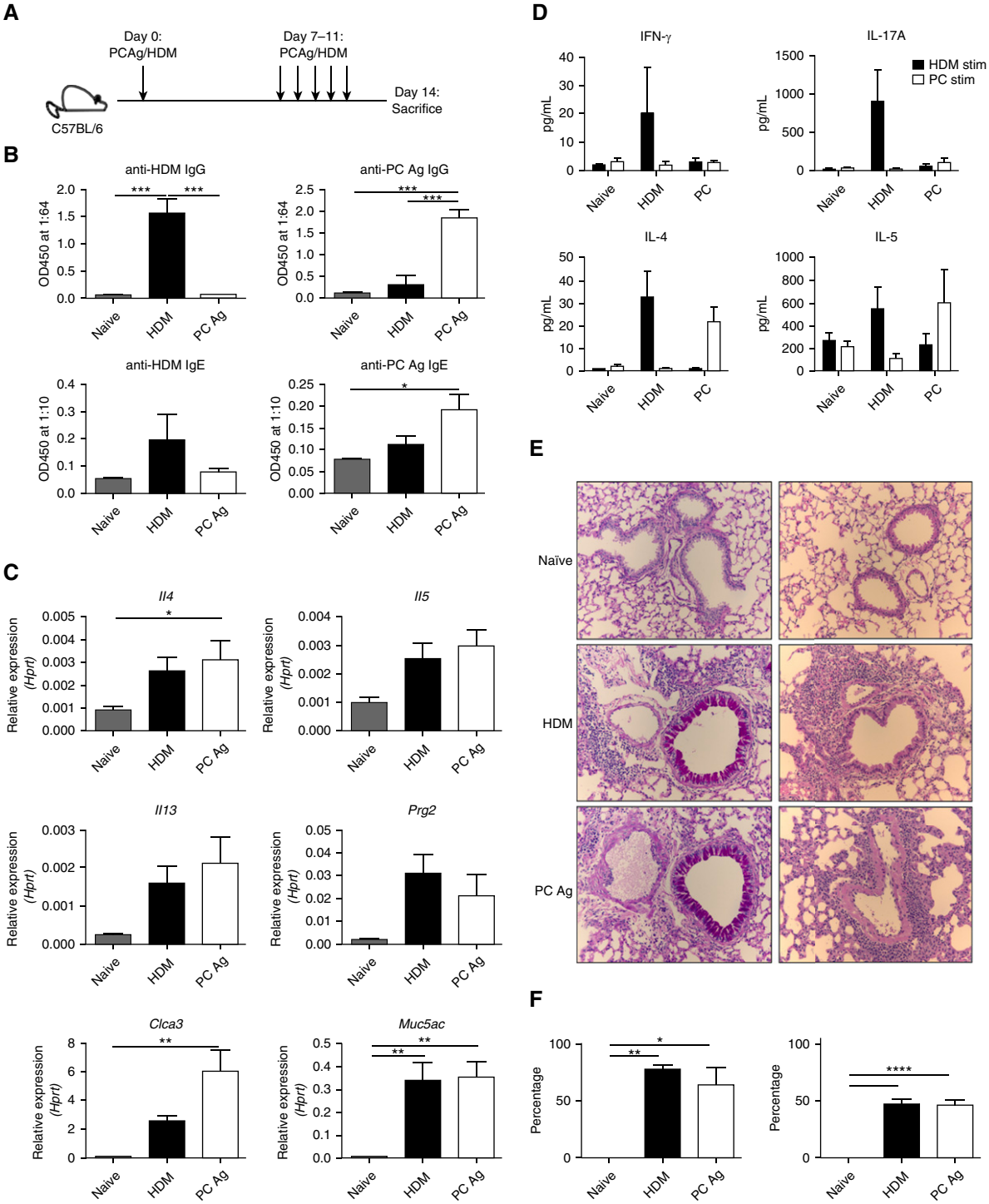

Figure 3. Exposure to *Pneumocystis* antigen (PCAg) and house dust mite (HDM) generates lung pathology. (*A*) Schematic of treatment of mice with 10 μg of HDM and sonicated PCAg on Days 0, 7, 8, 9, 10, and 11. Naive (n = 9), HDM (n = 6), and PCAg (n = 10) mice were all killed at Day 14. Data from three individual experiments are shown. (*B*) PCAg and HDM exposure generated anti-PC and anti-HDM IgG and IgE responses, respectively. (*C*) PCAg and HDM increased expression of type II–related genes, as determined by quantitative reverse transcriptase–polymerase chain reaction. (*D*) *Ex vivo* cells isolated from whole lung were stimulated with either HDM or PCAg for 72 hours, and supernatants were analyzed for IL-4, IL-5, IL-17A, and IFN-γ. (*E*) Representative periodic acid–Schiff and hematoxylin and eosin staining of tissue from naive, HDM-treated, and PCAg-treated mice demonstrating increased mucus and perivascular inflammation in the HDM and PCAg groups. All images were taken at ×20 original magnification. (*F*) HDM and PCAg treatment increased the percentage of total airways affected by mucus (*left*) and the area of individual airway periodic acid–Schiff–positive staining (*right*) (*$P < 0.05$, **$P < 0.01$, ***$P < 0.001$, and ****$P < 0.0001$ by one-way analysis of variance with Tukey's multiple comparisons). *Hprt* = hypoxanthine phosphoribosyltransferase; OD450 = optical density at 450 nm.

(Figure 2D), while PCAg exposure induced an antigen-specific release of IL-4 and IL-5 but not IL-17A (Figure 3D). Furthermore, PCAg-treated mice had an increase in antigen-specific $CD4^+$ Th2 cells as measured by upregulation of *Gata3* and increased expression of *Il4*, *Il5*, and *Il13* upon *ex vivo* stimulation with PCAg (Figure E3 in the online supplement). In concordance with the increased Th2 response, eosinophils were significantly increased following PCAg treatment (Figure E3 in the online supplement). PCAg treatment did not induce Th17 cells (as measured by RAR-related orphan receptor γT expression) or neutrophil recruitment (Figure E3 in the online supplement), however. Additionally, both PCAg- and HDM-treated mice had a striking upregulation of mucus production and increased perivascular inflammation on histologic sections (Figures 3E and 3F).

To assess functional changes in airway physiology, BALB/c mice were treated with PCAg or HDM. Quasistatic lung compliance was decreased with both PCAg and HDM treatment, indicative of inflammation in the lungs (Figure 4A). Similarly, both PCAg- and HDM-treated mice had significant increases in airway resistance compared with control animals when challenged with methacholine (Figure 4B). PCAg and HDM treatment also similarly increased parameters associated with parenchymal resistance (tissue damping) and recoil (tissue elastance) compared with naive mice (Figure 4C). As seen previously in C57BL/6 mice, both PCAg and HDM exposure increased expression of type II cytokines, mucus-associated genes, and *Prg2* in BALB/c mice in an equivalent manner (*see* Figure E4 in the online supplement).

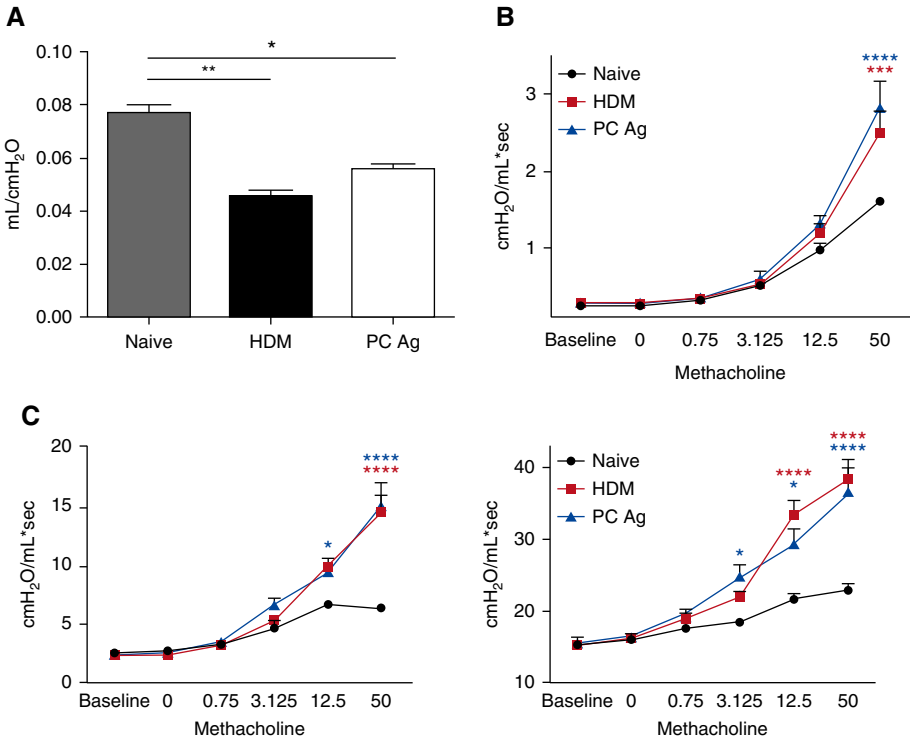

Figure 4. *Pneumocystis* antigen (PCAg) and house dust mite (HDM) comparably reduce lung function. BALB/c mice (n = 6 per group) were treated with either HDM or PCAg on Days 0 and 7–11 and were killed on Day 14. Naive BALB/c mice (n = 3) were analyzed as controls. Data represent the combination of two independent experiments. (*A*) Following anesthetization, tracheotomized mice were ventilated and quasistatic compliance was calculated using pressure–volume curves. BALB/c mice treated with HDM and PCAg had reduced compliance (*$P < 0.05$ and **$P < 0.01$ by one-way analysis of variance [ANOVA] with Tukey's multiple comparisons). (*B*) Newtonian airway resistance was calculated following escalating doses of aerosolized methacholine (0, 0.075, 3.125, 12.5, and 50 mg/ml). PCAg- and HDM-treated mice had increased resistance at higher doses of methacholine compared with naive BALB/c mice (***$P < 0.001$ and ****$P < 0.0001$ by two-way ANOVA with multiple comparisons). (*C*) Parameters associated with alveolar pathology (e.g., increased damping or elastance) were measured following treatment with methacholine and were also increased in PCAg- and HDM-treated mice (*$P < 0.05$ and ****$P < 0.0001$ by two-way ANOVA with multiple comparisons).

The Pathologic Response to PCAg Requires $CD4^+$ T Cells and Collaboration with ILC2 Cells

We next sought to determine the role of $CD4^+$ T cells and ILC2 cells in response to PCAg. As expected, anti-PC IgG and IgE production were decreased following $CD4^+$ depletion (Figure 5A). Furthermore, $CD4^+$ depletion significantly reduced expression of type II cytokines (*Il4* and *Il13*) as well as eosinophil genes (*Prg2*) and mucus-associated genes (*Muc5ac* and *Clca3*) (Figure 5B). $CD4^+$ depletion also significantly reduced PAS-positive airways, indicative of mucus production (Figures 5C and 5D).

To assess the role of ILC2 cells as effector cells contributing to allergic inflammation, the response to PCAg treatment was also observed in *Rag1*$^{-/-}$ mice, which lack T and B cells, or in *Rag2*$^{-/-}$*Il2rg*$^{-/-}$ mice, which lack adaptive immunity as well as natural killer cells and ILC2 cells. Further, *Rag1*$^{-/-}$ mice treated with PCAg were also treated with anti-ST2 antibody, which has been shown to neutralize the IL-33/ST2 signaling pathway and ILC2 expansion (39, 40). No significant induction in type II cytokines was observed in *Rag1*$^{-/-}$ or *Rag2*$^{-/-}$*Il2rg*$^{-/-}$ mice treated with PCAg (Figure 5B). *Rag1*$^{-/-}$ did have a small increase in mucus production that was ameliorated with anti-ST2 treatment, suggesting that ILC2 cells may have a minor role in inducing mucus-associated pathology (Figures 5C and 5D). These results demonstrate that $CD4^+$ T cells, and not ILC2 cells, are the primary effector cells responsible for the asthma-like pathology observed following PCAg treatment.

However, to assess the role of ILC2 cells upstream of the T-cell responses, C57BL/6 mice were exposed to PCAg and treated with anti-ST2 antibody. PCAg treatment did result in a small expansion of ILC2 cells that was neutralized by anti-ST2 treatment (*see* Figure E5 in the online supplement). However, in addition to impairing ILC2 expansion, blockade of ST2 reduced the percentage of $GATA3^+$ Th2 cells (*see* Figure E5 in the online supplement). Anti-ST2 treatment did not impair production of

anti-PC IgG or IgE, but it did reduce expression of type II cytokines (*Il4, Il5*, and *Il13*) and an eosinophil-specific marker, *Prg2* (*see* Figure E5 in the online supplement). However, anti-ST2 treatment was insufficient to reduce the mucus response as measured by quantitative reverse transcriptase–polymerase chain reaction and PAS staining of the airways (*see* Figure E5 in the online supplement). Taken together, the results of these studies demonstrate that the IL-33/ST2 pathway is required for expansion of ILC2 and Th2 cells in response to PCAg. Further, these results are suggestive that ILC2 cells may influence the Th2 response but do not play a significant role in driving the lung pathology induced by PCAg.

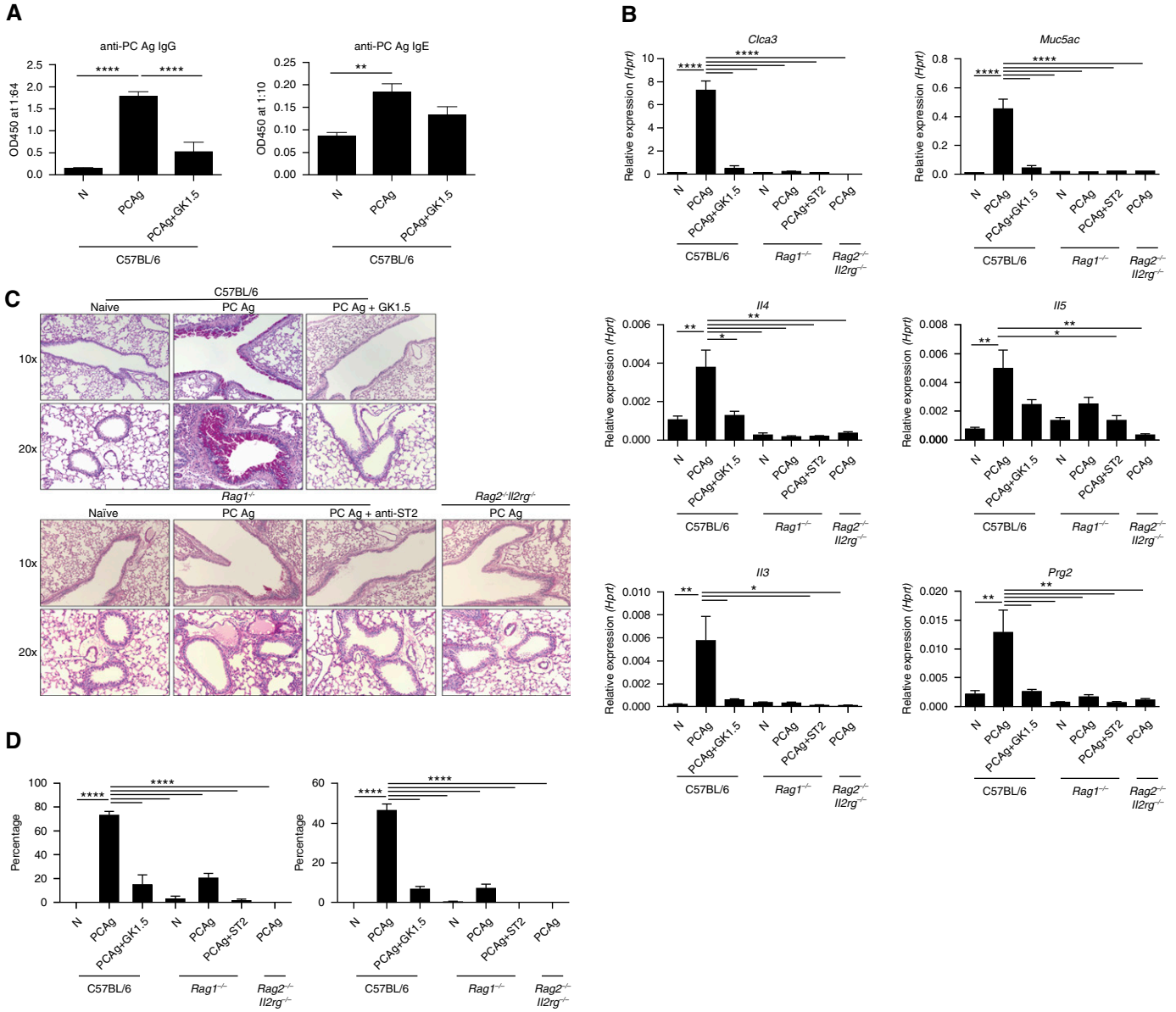

Figure 5. CD4$^+$ T cells, but not type II innate lymphoid (ILC2) cells, are the primary effectors of *Pneumocystis* antigen (PCAg)–driven pathology. C57BL/6 mice (n = 6 per group) were untreated, treated with PCAg, or treated with both PCAg and GK1.5 monoclonal antibody and killed at Day 14. Data represent the combination of two independent experiments. Naive *Rag1*$^{-/-}$ mice (n = 3), *Rag1*$^{-/-}$ mice treated with PCAg (n = 3), *Rag1*$^{-/-}$ mice treated with anti-ST2 antibody and PCAg (n = 4), and *Rag2*$^{-/-}$*Il2rg*$^{-/-}$ mice treated with PCAg (n = 3) were also analyzed. (*A*) Anti-*Pneumocystis* (anti-PC) antibody production (IgG and IgE) is dependent on CD4$^+$ T cells. (*B*) Expression of type II immune response genes in whole-lung homogenate at Day 14 appears to be mediated by CD4$^+$ T cells but not ILC2 cells. (*C*) Periodic acid–Schiff staining of whole lung shows that CD4$^+$ T cells drive the mucus response to PCAg, while limited ILC2-dependent mucus production was noted in *Rag1*$^{-/-}$ mice. (*D*) PCAg treatment significantly increased the percentage of total airways affected by mucus (*left*) and the area of individual airway periodic acid–Schiff–positive staining (*right*) in a CD4-dependent manner (*$P < 0.05$, **$P < 0.01$, and ****$P < 0.0001$ by one-way analysis of variance with Tukey's multiple comparisons). *Hprt* = hypoxanthine phosphoribosyltransferase; OD450 = optical density at 450 nm.

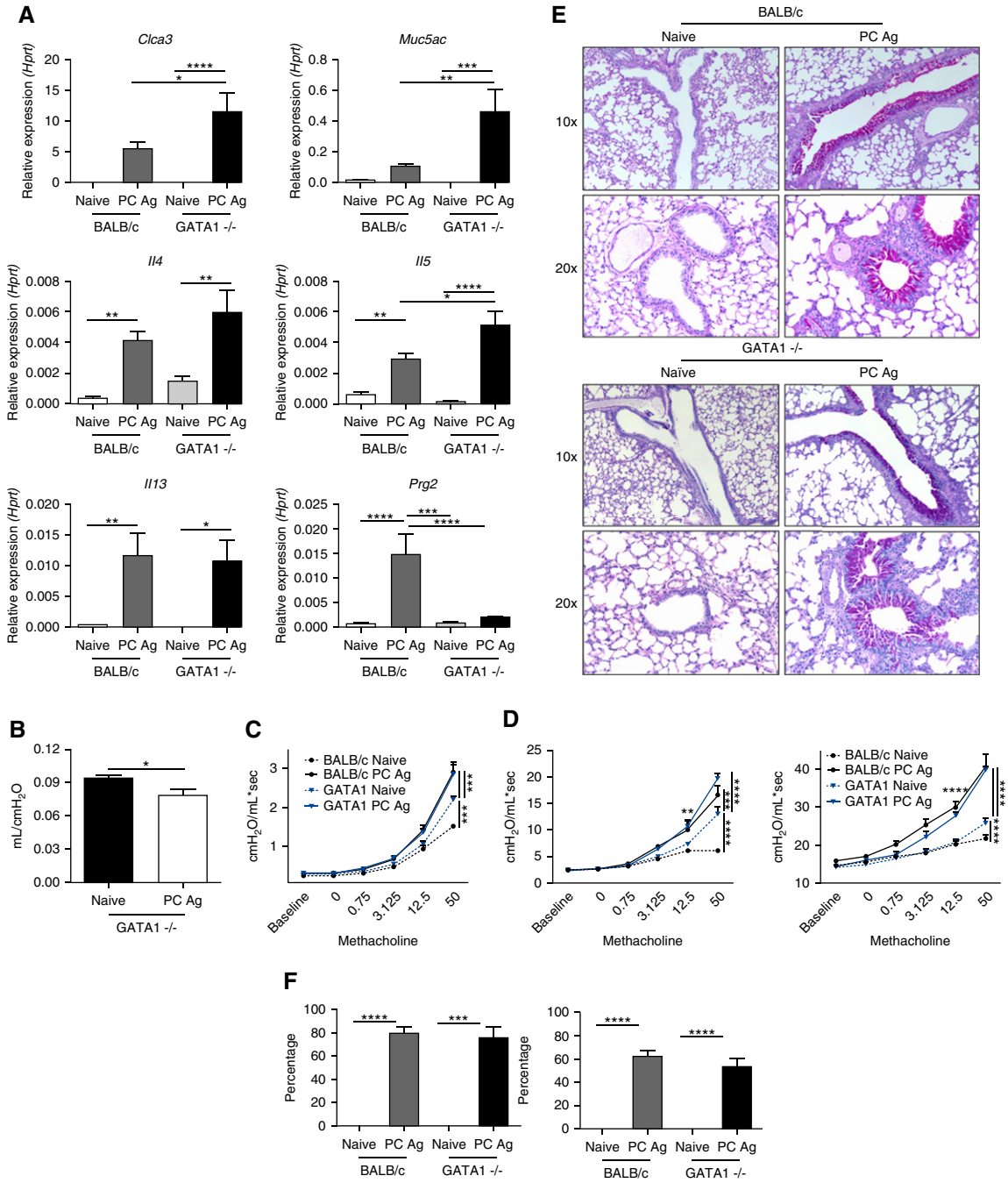

Figure 6. Eosinophils are dispensable for pathology following *Pneumocystis* antigen (PCAg) exposure. BALB/c and *GATA1*^{tm6Sho}*/J* mice were treated with PCAg (n = 5 for naive BALB/c, n = 8 BALB/c + PC Ag, n = 8 for *GATA1*^{tm6Sho}*/J*) and killed at Day 14. Data represent the combination of two independent experiments. (*A*) RNA isolated from lung homogenate demonstrates that *GATA1*^{tm6Sho}*/J* mice are capable of mounting a type II response comparable to, if not greater than, that of BALB/c mice (*$P < 0.05$, **$P < 0.01$, ***$P < 0.001$, and ****$P < 0.0001$ by one-way analysis of variance [ANOVA] with Tukey's multiple comparisons). (*B*) Following anesthetization, tracheotomized mice were ventilated and quasistatic compliance was calculated using pressure–volume curves. *GATA1*^{tm6Sho}*/J* mice treated with PCAg had reduced compliance (*$P < 0.05$ by Student's *t* test). (*C*) Newtonian airway resistance was calculated following escalating doses of aerosolized methacholine (0, 0.075, 3.125, 12.5, and 50 mg/ml). *GATA1*^{tm6Sho}*/J* mice, like BALB/c mice, had exacerbated airway resistance following PCAg treatment (***$P < 0.001$ by two-way ANOVA with multiple comparisons). (*D*) Tissue damping and tissue elastance were increased in *GATA1*^{tm6Sho}*/J* mice following PCAg treatment (**$P < 0.01$, ***$P < 0.001$, and ****$P < 0.0001$ by two-way ANOVA with multiple comparisons). (*E*) Periodic acid–Schiff staining of naive and PCAg BALB/c and *GATA1*^{tm6Sho}*/J* tissues demonstrates similar mucus production in both large and small airways in the PCAg-treated groups. (*F*) Quantification of periodic acid–Schiff staining demonstrates that BALB/c and *GATA1*^{tm6Sho}*/J* mice have equally affected airways following PCAg treatment (***$P < 0.001$ and ****$P < 0.0001$ by one-way ANOVA with Tukey's multiple comparisons). *Hprt* = hypoxanthine phosphoribosyltransferase.

Eosinophils Are Dispensable for PCAg-driven Pathology

We next sought to characterize the role of eosinophils in the pathologic response to PCAg. *GATA1*^{tm6Sho}*/J* mice treated with PCAg had increased *Clca3*, *Muc5ac*, *Il4*, *Il5*, and *Il13* compared with naive *GATA1*^{tm6Sho}*/J* mice (Figure 6A). Compared with BALB/c mice treated with PCAg, *GATA1*^{tm6Sho}*/J* mice had significant upregulation of *Clca3*, *Muc5ac*, and *Il5* but not *Prg2*. *GATA1*^{tm6Sho}*/J* mice also had a significant reduction in quasistatic compliance similar to that seen in BALB/c mice (Figure 6B). Furthermore, *GATA1*^{tm6Sho}*/J* mice had exacerbated airway resistance in the airways following PCAg compared with naive *GATA1*^{tm6Sho}*/J* mice (Figure 6C). Although there appeared to be an increase in airway resistance in naive *GATA1*^{tm6Sho}*/J* mice compared with naive BALB/c mice, PCAg-challenged *GATA1*^{tm6Sho}*/J* mice had significantly elevated airway resistance similar to that of challenged BALB/c mice. Significant changes in alveolar parameters were also observed following PCAg exposure in *GATA1*^{tm6Sho}*/J* mice (Figure 6D). Histologically, *GATA1*^{tm6Sho}*/J* mice had mucus production similar to that of BALB/c mice treated with PCAg (Figure 6E).

Patients with Severe Asthma Have Increased Antibody Titers to *Pneumocystis*

As prior studies have implicated PC as a ubiquitous environmental exposure, we sought to determine if differences in anti-PC antibodies correlated with asthma status. Patients with severe asthma (SA) had significantly elevated anti-PC IgG levels compared with healthy control subjects (HCs) (Figure 7A). Strikingly, a subset of patients with SA had elevated antibody levels, as several individual antibody titer curves were shifted to the right compared with those of the HCs (*see* Figure E6 in the online supplement). In Western blot analysis, samples from both a single HC subject and a single patient with SA appeared to recognize similar PC antigens; however, the sample from the patient with SA recognized these antigens with greater intensity, corroborating the ELISA findings (Figure 7B). Because of concerns about contaminating mouse proteins within the PCAg preparation, we probed mouse lung homogenate with the same human serum samples and found little reactivity (*see* Figure E7 in the online supplement). To assess the specificity of these antibody responses, we evaluated antibody production in response to another respiratory pathogen, *Streptococcus pneumoniae* (SP). Interestingly, patients with SA had significantly decreased anti-SP antibodies compared with HCs (Figure 7C). No antibody titer curve shifts to the right were observed in patients with SA in regard to anti-SP IgG (*see* Figure E6 in the online supplement). Additionally, as previously observed in the murine model of PC exposure, a subset of patients with SA had detectable anti-PC IgE levels (Figure 7D). A strong positive correlation between anti-PC IgG and IgE levels was observed, as patients with elevated anti-PC IgG were more likely to have increased anti-PC IgE levels as well (Figure 7E).

To rule out the possibility of nonspecific binding to fungal antigens, the serum samples were also assessed for anti-*Aspergillus* antibodies. We observed no difference between HCs and patients with SA in this analysis (Figures 7F and 7G). Further, no correlation existed between anti-PC and anti-*Aspergillus* IgG or IgE (Figures 7H and 7I).

Patients with Severe Asthma with Increased Anti-*Pneumocystis* Antibody Levels Have Worsened Symptomatology and Lung Function

We next stratified patients with SA into PC-high or PC-low subsets using a *z*-score approach. Any individual with an anti-PC IgG response above a *z*-score of 1 (2.02 based on the HC cohort) was considered PC-high (n = 11); a patient with an ELISA optical density of 2.02 or less was considered PC-low (n = 9) (Figure 8A). The PC-high group had a significantly older age than the PC-low group at the time of the study; other demographic data were similar (Figure 8A). The PC-low subset was 67% female and included 22% ever smokers, compared with 81% female and 36% ever smokers in the PC-high group.

Serum IgE levels for the PC-low and PC-high groups were comparable, and levels in both groups appeared elevated compared with those of HCs (*see* Figure E8 in the online supplement). Importantly, there did not appear to be a difference between groups in allergen skin test results (*see* Figure E8 in the online supplement). Additionally, there were no differences in blood neutrophils, lymphocytes, or eosinophils between the PC-high and PC-low patients (*see* Figure E9 in the online supplement). Similar cell counts were also observed in bronchoalveolar lavage (*see* Figure E9 in the online supplement). There were also no observed differences in inhaled or oral steroid use or steroid doses between the PC-high and PC-low groups (data not shown).

The subset of patients with SA in the PC-high group had worsened symptom scores compared with the patients with SA in the PC-low group with regard to cough, as well as a trend toward increased shortness of breath (Figure 8B). Interestingly, patients with SA in the PC-high group had a trend toward reduced sputum production compared with the patients with SA in the PC-low group (Figure 8B). Spirometry revealed that PC-high patients had significantly decreased FEV_1 and a trend toward decreased FVC and forced expiratory flow 25–75% (Figure 8C). Patients with SA in the PC-high group also had increased air trapping as determined by plethysmography, as PC-high patients (n = 7) had increased total lung capacity and residual volume compared with PC-low SA patients (n = 9) (Figure 8D).

Discussion

The results of the present study demonstrate, for the first time to our knowledge, that PC infection and antigen treatment induce an asthma-like pathologic response in the lung driven by $CD4^+$ T cells. The ability of PC to induce a strong Th2 response may have implications in immunocompetent patients, as it has recently been shown that the majority of healthy individuals have detectable anti-PC antibodies (26). Furthermore, colonization of live PC within the lung may occur as a transitional state of low PC burden, with the specific host–pathogen interactions (e.g., immunosuppression) ultimately determining the differences between disease, colonization, and clearance (23). Indeed, asymptomatic infection with PC may have immunologic ramifications, as infants with detectable PC in the lungs were previously found to have increased mucus production (21, 41), consistent with the findings in our murine model.

The ubiquity of human exposure to PC and the specific nature of the immune response to PC beg the question of how this pathogen and the subsequent host response may impact asthma. Researchers in one prior study demonstrated that PC could worsen an ovalbumin murine model of asthma by altering dendritic cell subsets (38). While concurrent PC infection only slightly modified an HDM model in the present study, PC appeared to prime an equally potent type II response compared with mice treated with HDM alone. These findings, coupled with the PCAg model, suggest that, much like HDM, PC functions as an airway allergen (42, 43). Much like what has been shown previously with HDM, PCAg further exacerbated airway responsiveness in *GATA1*^{tm6Sho}*/J* mice (44, 45). The necessity of eosinophils in mediating airway hyperresponsiveness has been difficult to demonstrate definitively, though, as variations between a knockout mouse model and an antigenic model have shown differing outcomes (46, 47).

There were some unique differences between the HDM and PCAg models. ILC2 cells have been shown to be prolific producers of type II cytokines in response to both pulmonary and intradermal HDM exposure (48, 49). Similarly, murine models of fungal allergen exposure to *Alternaria* have also demonstrated a role for ILC2 cells as cytokine producers (50, 51). In the present PC model, ILC2 cells appeared to have a greater function in maintaining the optimal Th2 response as opposed to directly contributing to pathology via cytokine production. This priming function has been shown previously to require major histocompatibility complex class II

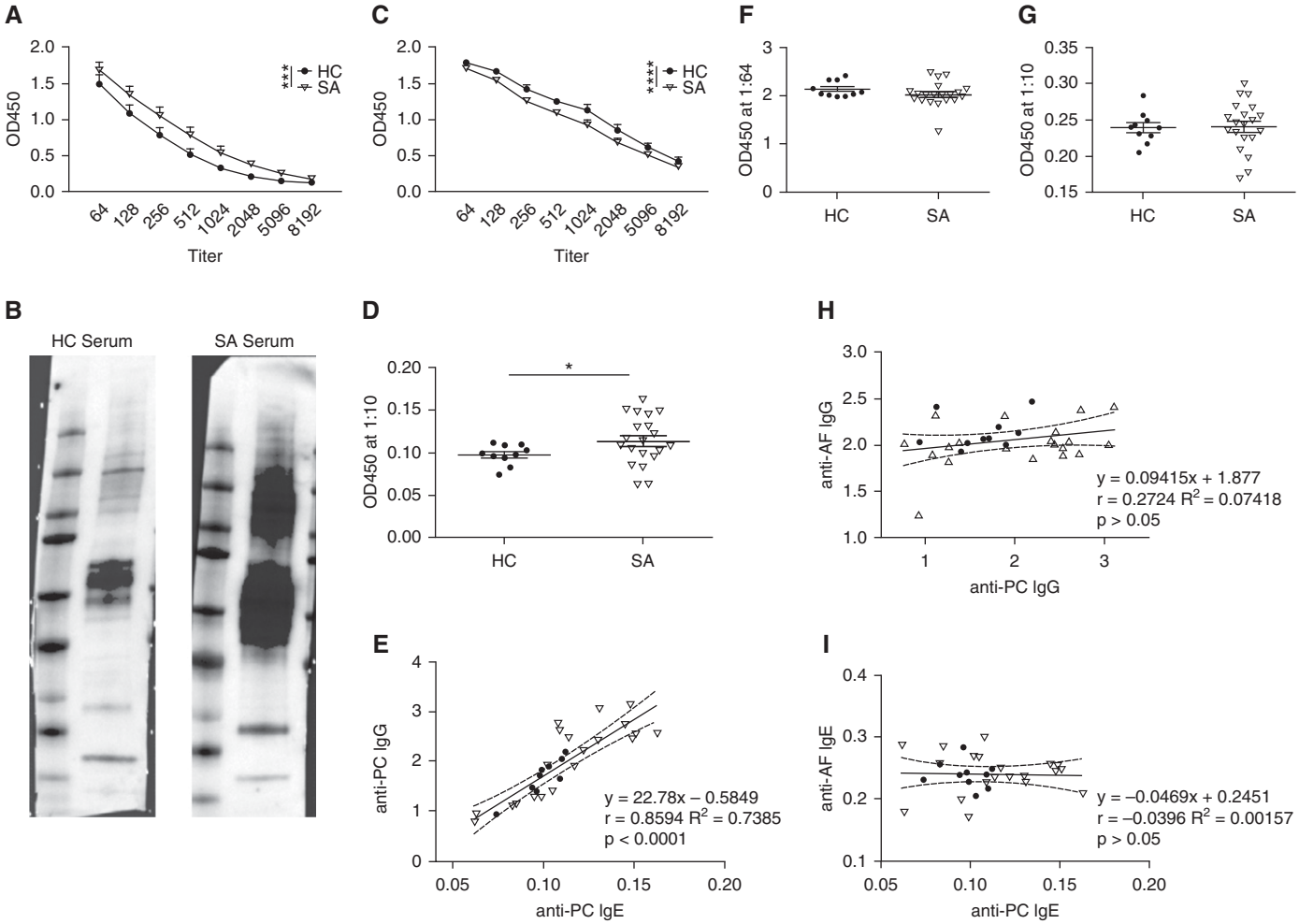

Figure 7. Patients with severe asthma have elevated anti-*Pneumocystis* (anti-PC) IgG and IgE levels. (*A*) Serum samples from healthy control subjects (HC) (n = 10) and patients with severe asthma (SA) (n = 20) were analyzed for anti-PC IgG at various dilutions. Patients with SA had increased antibody levels against PC (***$P < 0.001$ by two-way analysis of variance). (*B*) Detection of anti-PC IgG from one HC and one patient with SA demonstrates similar banding patterns but increased intensity in the patient with SA. (*C*) Serum samples from HCs and patients with SA were also analyzed for IgG levels against *Streptococcus pneumoniae*, and patients with SA had reduced antibody levels (****$P < 0.0001$ by two-way analysis of variance). (*D*) Anti-PC IgE could be detected by ELISA in the serum (diluted 1:10) of a subset of patients with SA (*$P < 0.05$ by Student's *t* test). (*E*) Linear regression and Pearson's correlation analysis demonstrates a strong correlation between anti-PC IgG and anti-PC IgE levels in all patients ($r = 0.8594$; $P < 0.0001$). (*F* and *G*) Patients with SA do not have an increase in (*F*) anti-*Aspergillus* IgG or (*G*) anti-*Aspergillus* IgE. (*H*) No correlation exists between anti-PC IgG and anti-*Aspergillus* IgG ($r = 0.2724$; $P > 0.05$). (*I*) No correlation exists between anti-PC IgE and anti-*Aspergillus* IgE ($r = -0.0396$; $P > 0.05$). AF = *Aspergillus fumigatus*; OD450 = optical density at 450 nm.

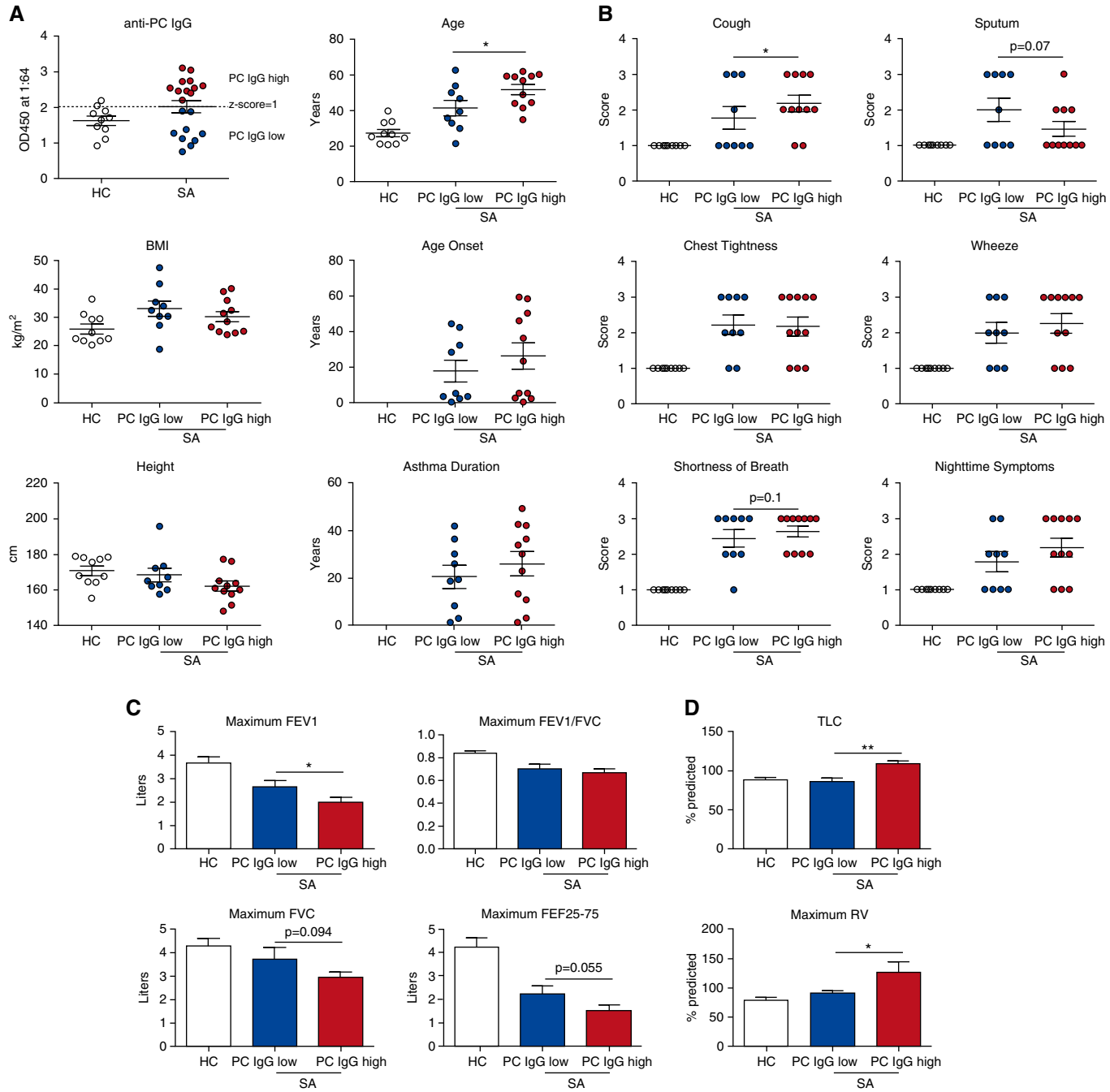

Figure 8. Patients with severe asthma (SA) with increased anti-*Pneumocystis* (anti-PC) IgG have worsened symptoms and decreased lung function. (*A*) Patients with SA were stratified into PC-high (n = 11) and PC-low (n = 9) groups by using a *z*-score of 1 in the healthy control (HC) population, with an optical density at 450 nm (OD450) of 2.02 serving as the cutoff (*dashed line*). The demographics for these patient populations were similar, with the exception of age; PC-high patients were significantly older (*$P < 0.05$ by Student's *t* test). (*B*) Symptomatology as reported by the patients in answering a standard questionnaire shows PC-high patients having increased symptom severity in every symptom except for sputum production (*$P < 0.05$ by χ^2 analysis). (*C*) Spirometric assessment of lung function demonstrates PC-high patients had decreased FEV_1 (*$P < 0.05$ by Student's *t* test) and trends toward decreased FVC and forced expiratory flow 25–75% (FEF25–75) compared with PC-low patients. (*D*) Plethysmography demonstrates PC-high patients had increased total lung capacity (TLC) and residual volume (RV) compared with PC-low patients (*$P < 0.05$ and **$P < 0.01$ by Student's *t* test). BMI = body mass index.

expression on ILC2 cells, although it is unclear if direct antigen presentation is required in the PCAg model (52, 53). One further difference between the HDM and PCAg models appears to be the specificity of the respective antigens and antibody responses. The antigen-specific recall responses and antibody responses to PCAg and HDM did not cross react, suggesting that distinct antigens, and not molecular patterns such as chitin, are recognized in these two models (54, 55).

While evidence in the mouse model shows that PC infection and exposure can lead to lung pathology, this has yet to be studied formally in a population of immunocompetent patients with asthma. Researchers in one study found an association between HIV-positive patients with prior pneumonia with either PC or a bacterial pathogen and doctor-diagnosed asthma (56). A second study of HIV-positive individuals demonstrated that history of PC was associated with an obstructed spirometric pattern in lung function testing (57). While these prior studies were focused on fulminant infection in an HIV-positive host, in the present study we examined immune exposure by measuring anti-PC antibody levels in the blood of patients with or without asthma. Strikingly, compared with HCs, a cohort of patients with SA had elevated anti-PC IgG and IgE antibodies in their serum. Importantly, this did not appear to be a result of nonspecific immune activation in response to all pathogens, as patients with SA had decreased antibody responses to *S. pneumoniae* and similar antibody responses to *Aspergillus* compared with HCs. These findings are suggestive of increased exposure to PC in patients with SA compared with healthy individuals; whether this exposure represents persistent colonization or transient contact with airborne spores is unclear. One possibility is that this increase in PC exposure is due to the use of both inhaled and oral corticosteroids in patients with SA (58).

Thus, the present study cannot differentiate a model where PC exposure increases the likelihood of developing SA from a model where patients with SA are more likely to be exposed to PC as a result of steroid exposure. Monitoring PC colonization status using molecular techniques could be useful in understanding the effects of local immunosuppression on PC colonization, and such techniques could be applied longitudinally in a healthy human cohort to assess the development of asthma.

Importantly, in the present study, we identified the presence of anti-PC IgE in serum samples of patients with asthma. Type I hypersensitivity to PC, therefore, may be diagnosed much like that of other allergens routinely tested in the clinical setting. This also raises the exciting possibility of intervening with trimethoprim-sulfamethoxazole, the hallmark of treatment and prophylaxis for PC, in patients with SA with known sensitization and/or colonization with PC. While further studies elucidating the interplay between PC and asthma are essential to informing future clinical investigations, the present study demonstrates that, in both a murine model and human patients, PC may lead to the development of lung pathology and thus a clinical phenotype similar to asthma. ■

Author disclosures are available with the text of this article at www.atsjournals.org.

Acknowledgment: T.E. acknowledges Dr. Allyson Larkin and Dr. Geoffrey Kurland for clinical mentorship and guidance. The authors acknowledge John Trudeau for his ongoing help with the Severe Asthma Research Program. The authors also thank Dr. Dirk Smith for generously providing the anti-ST2 antibody. In addition, the authors acknowledge Dr. Stokes Peebles at Vanderbilt University for critical analysis of the manuscript during its preparation.

References

1. Jackson DJ, Sykes A, Mallia P, Johnston SL. Asthma exacerbations: origin, effect, and prevention. *J Allergy Clin Immunol* 2011;128:1165–1174.
2. Braman SS. The global burden of asthma. *Chest* 2006;130(1, Suppl): 4S–12S.
3. Kim HY, DeKruyff RH, Umetsu DT. The many paths to asthma: phenotype shaped by innate and adaptive immunity. *Nat Immunol* 2010;11:577–584.
4. Moore WC, Meyers DA, Wenzel SE, Teague WG, Li H, Li X, D'Agostino R Jr, Castro M, Curran-Everett D, Fitzpatrick AM, *et al*.; National Heart, Lung, and Blood Institute's Severe Asthma Research Program. Identification of asthma phenotypes using cluster analysis in the Severe Asthma Research Program. *Am J Respir Crit Care Med* 2010;181:315–323.
5. Ray A, Oriss TB, Wenzel SE. Emerging molecular phenotypes of asthma. *Am J Physiol Lung Cell Mol Physiol* 2015;308:L130–L140.
6. Wesolowska-Andersen A, Seibold MA. Airway molecular endotypes of asthma: dissecting the heterogeneity. *Curr Opin Allergy Clin Immunol* 2015;15:163–168.
7. Erle DJ, Sheppard D. The cell biology of asthma. *J Cell Biol* 2014;205: 621–631.
8. Lambrecht BN, Hammad H. The immunology of asthma. *Nat Immunol* 2015;16:45–56.
9. Moffatt MF, Gut IG, Demenais F, Strachan DP, Bouzigon E, Heath S, von Mutius E, Farrall M, Lathrop M, Cookson WO; GABRIEL Consortium. A large-scale, consortium-based genomewide association study of asthma. *N Engl J Med* 2010;363:1211–1221.
10. Wu P, Hartert TV. Evidence for a causal relationship between respiratory syncytial virus infection and asthma. *Expert Rev Anti Infect Ther* 2011;9:731–745.
11. Schauer U, Hoffjan S, Bittscheidt J, Köchling A, Hemmis S, Bongartz S, Stephan V. RSV bronchiolitis and risk of wheeze and allergic sensitisation in the first year of life. *Eur Respir J* 2002;20: 1277–1283.
12. Hammad H, Lambrecht BN. Barrier epithelial cells and the control of type 2 immunity. *Immunity* 2015;43:29–40.
13. Vicencio AG, Santiago MT, Tsirilakis K, Stone A, Worgall S, Foley EA, Bush D, Goldman DL. Fungal sensitization in childhood persistent asthma is associated with disease severity. *Pediatr Pulmonol* 2014;49:8–14.
14. Denning DW, O'Driscoll BR, Hogaboam CM, Bowyer P, Niven RM. The link between fungi and severe asthma: a summary of the evidence. *Eur Respir J* 2006;27:615–626.
15. Edwards MR, Bartlett NW, Hussell T, Openshaw P, Johnston SL. The microbiology of asthma. *Nat Rev Microbiol* 2012;10:459–471.
16. Doherty TA, Khorram N, Sugimoto K, Sheppard D, Rosenthal P, Cho JY, Pham A, Miller M, Croft M, Broide DH. *Alternaria* induces STAT6-dependent acute airway eosinophilia and epithelial FIZZ1 expression that promotes airway fibrosis and epithelial thickness. *J Immunol* 2012;188:2622–2629.
17. Kheradmand F, Kiss A, Xu J, Lee SH, Kolattukudy PE, Corry DB. A protease-activated pathway underlying Th cell type 2 activation and allergic lung disease. *J Immunol* 2002;169:5904–5911.
18. Eddens T, Kolls JK. Pathological and protective immunity to *Pneumocystis* infection. *Semin Immunopathol* 2015;37:153–162.
19. Morris A, Lundgren JD, Masur H, Walzer PD, Hanson DL, Frederick T, Huang L, Beard CB, Kaplan JE. Current epidemiology of *Pneumocystis* pneumonia. *Emerg Infect Dis* 2004;10:1713–1720.
20. Mikaelsson L, Jacobsson G, Andersson R. *Pneumocystis* pneumonia – a retrospective study 1991–2001 in Gothenburg, Sweden. *J Infect* 2006;53:260–265.
21. Vargas SL, Ponce CA, Gallo M, Pérez F, Astorga JF, Bustamante R, Chabé M, Durand-Joly I, Iturra P, Miller RF, *et al*. Near-universal prevalence of *Pneumocystis* and associated increase in mucus in the lungs of infants with sudden unexpected death. *Clin Infect Dis* 2013; 56:171–179.
22. Probst M, Ries H, Schmidt-Wieland T, Serr A. Detection of *Pneumocystis carinii* DNA in patients with chronic lung diseases. *Eur J Clin Microbiol Infect Dis* 2000;19:644–645.

23. Morris A, Wei K, Afshar K, Huang L. Epidemiology and clinical significance of *Pneumocystis* colonization. *J Infect Dis* 2008;197: 10–17.
24. Fitzpatrick ME, Tedrow JR, Hillenbrand ME, Lucht L, Richards T, Norris KA, Zhang Y, Sciurba FC, Kaminski N, Morris A. *Pneumocystis jirovecii* colonization is associated with enhanced Th1 inflammatory gene expression in lungs of humans with chronic obstructive pulmonary disease. *Microbiol Immunol* 2014;58: 202–211.
25. Morris A, Norris KA. Colonization by *Pneumocystis jirovecii* and its role in disease. *Clin Microbiol Rev* 2012;25:297–317.
26. Respaldiza N, Medrano FJ, Medrano AC, Varela JM, de la Horra C, Montes-Cano M, Ferrer S, Wichmann I, Gargallo-Viola D, Calderon EJ. High seroprevalence of *Pneumocystis* infection in Spanish children. *Clin Microbiol Infect* 2004;10:1029–1031.
27. Centers for Disease Control (CDC). *Pneumocystis* pneumonia—Los Angeles. *MMWR Morb Mortal Wkly Rep* 1981;30:250–252.
28. Beck JM, Warnock ML, Curtis JL, Sniezek MJ, Arraj-Peffer SM, Kaltreider HB, Shellito JE. Inflammatory responses to *Pneumocystis carinii* in mice selectively depleted of helper T lymphocytes. *Am J Respir Cell Mol Biol* 1991;5:186–197.
29. Elsegeiny W, Eddens T, Chen K, Kolls JK. Anti-CD20 antibody therapy and susceptibility to *Pneumocystis* pneumonia. *Infect Immun* 2015; 83:2043–2052.
30. Opata MM, Hollifield ML, Lund FE, Randall TD, Dunn R, Garvy BA, Feola DJ. B lymphocytes are required during the early priming of $CD4^+$ T cells for clearance of *Pneumocystis* infection in mice. *J Immunol* 2015;195:611–620.
31. Eddens T, Elsegeiny W, Nelson MP, Horne W, Campfield BT, Steele C, Kolls JK. Eosinophils contribute to early clearance of *Pneumocystis murina* infection. *J Immunol* 2015;195:185–193.
32. Zheng M, Shellito JE, Marrero L, Zhong Q, Julian S, Ye P, Wallace V, Schwarzenberger P, Kolls JK. $CD4^+$ T cell–independent vaccination against *Pneumocystis carinii* in mice. *J Clin Invest* 2001;108:1469–1474.
33. Zheng M, Ramsay AJ, Robichaux MB, Kliment C, Crowe C, Rapaka RR, Steele C, McAllister F, Shellito JE, Marrero L, *et al*. $CD4^+$ T cell–independent DNA vaccination against opportunistic infections. *J Clin Invest* 2005;115:3536–3544.
34. Manni ML, Trudeau JB, Scheller EV, Mandalapu S, Elloso MM, Kolls JK, Wenzel SE, Alcorn JF. The complex relationship between inflammation and lung function in severe asthma. *Mucosal Immunol* 2014;7:1186–1198.
35. Alcorn JF, Rinaldi LM, Jaffe EF, van Loon M, Bates JH, Janssen-Heininger YM, Irvin CG. Transforming growth factor-β1 suppresses airway hyperresponsiveness in allergic airway disease. *Am J Respir Crit Care Med* 2007;176:974–982.
36. Hantos Z, Daróczy B, Suki B, Nagy S, Fredberg JJ. Input impedance and peripheral inhomogeneity of dog lungs. *J Appl Physiol (1985)* 1992;72:168–178.
37. Tomioka S, Bates JH, Irvin CG. Airway and tissue mechanics in a murine model of asthma: alveolar capsule vs. forced oscillations. *J Appl Physiol (1985)* 2002;93:263–270.
38. Swain SD, Meissner N, Han S, Harmsen A. *Pneumocystis* infection in an immunocompetent host can promote collateral sensitization to respiratory antigens. *Infect Immun* 2011;79:1905–1914.
39. Sedhom MA, Pichery M, Murdoch JR, Foligné B, Ortega N, Normand S, Mertz K, Sanmugalingam D, Brault L, Grandjean T, *et al*. Neutralisation of the interleukin-33/ST2 pathway ameliorates experimental colitis through enhancement of mucosal healing in mice. *Gut* 2013;62:1714–1723.
40. Monticelli LA, Sonnenberg GF, Abt MC, Alenghat T, Ziegler CG, Doering TA, Angelosanto JM, Laidlaw BJ, Yang CY, Sathaliyawala T, *et al*. Innate lymphoid cells promote lung-tissue homeostasis after infection with influenza virus. *Nat Immunol* 2011;12:1045–1054.
41. Pérez FJ, Ponce CA, Rojas DA, Iturra PA, Bustamante RI, Gallo M, Hananias K, Vargas SL. Fungal colonization with *Pneumocystis* correlates to increasing chloride channel accessory 1 (hCLCA1) suggesting a pathway for up-regulation of airway mucus responses, in infant lungs. *Results Immunol* 2014;4:58–61.
42. Gregory LG, Causton B, Murdoch JR, Mathie SA, O'Donnell V, Thomas CP, Priest FM, Quint DJ, Lloyd CM. Inhaled house dust mite induces pulmonary T helper 2 cytokine production. *Clin Exp Allergy* 2009;39: 1597–1610.
43. Johnson JR, Wiley RE, Fattouh R, Swirski FK, Gajewska BU, Coyle AJ, Gutierrez-Ramos JC, Ellis R, Inman MD, Jordana M. Continuous exposure to house dust mite elicits chronic airway inflammation and structural remodeling. *Am J Respir Crit Care Med* 2004;169:378–385.
44. Fattouh R, Al-Garawi A, Fattouh M, Arias K, Walker TD, Goncharova S, Coyle AJ, Humbles AA, Jordana M. Eosinophils are dispensable for allergic remodeling and immunity in a model of house dust mite-induced airway disease. *Am J Respir Crit Care Med* 2011;183:179–188.
45. Tournoy KG, Kips JC, Schou C, Pauwels RA. Airway eosinophilia is not a requirement for allergen-induced airway hyperresponsiveness. *Clin Exp Allergy* 2000;30:79–85.
46. Humbles AA, Lloyd CM, McMillan SJ, Friend DS, Xanthou G, McKenna EE, Ghiran S, Gerard NP, Yu C, Orkin SH, *et al*. A critical role for eosinophils in allergic airways remodeling. *Science* 2004;305:1776–1779.
47. Lee JJ, Dimina D, Macias MP, Ochkur SI, McGarry MP, O'Neill KR, Protheroe C, Pero R, Nguyen T, Cormier SA, *et al*. Defining a link with asthma in mice congenitally deficient in eosinophils. *Science* 2004; 305:1773–1776.
48. Klein Wolterink RG, Kleinjan A, van Nimwegen M, Bergen I, de Bruijn M, Levani Y, Hendriks RW. Pulmonary innate lymphoid cells are major producers of IL-5 and IL-13 in murine models of allergic asthma. *Eur J Immunol* 2012;42:1106–1116.
49. Salimi M, Barlow JL, Saunders SP, Xue L, Gutowska-Owsiak D, Wang X, Huang LC, Johnson D, Scanlon ST, McKenzie AN, *et al*. A role for IL-25 and IL-33-driven type-2 innate lymphoid cells in atopic dermatitis. *J Exp Med* 2013;210:2939–2950.
50. Oczypok EA, Milutinovic PS, Alcorn JF, Khare A, Crum LT, Manni ML, Epperly MW, Pawluk AM, Ray A, Oury TD. Pulmonary receptor for advanced glycation end-products promotes asthma pathogenesis through IL-33 and accumulation of group 2 innate lymphoid cells. *J Allergy Clin Immunol* 2015;136:747–756.e4.
51. Snelgrove RJ, Gregory LG, Peiró T, Akthar S, Campbell GA, Walker SA, Lloyd CM. Alternaria-derived serine protease activity drives IL-33-mediated asthma exacerbations. *J Allergy Clin Immunol* 2014;134: 583–592.e6.
52. Oliphant CJ, Hwang YY, Walker JA, Salimi M, Wong SH, Brewer JM, Englezakis A, Barlow JL, Hams E, Scanlon ST, *et al*. MHCII-mediated dialog between group 2 innate lymphoid cells and $CD4^+$ T cells potentiates type 2 immunity and promotes parasitic helminth expulsion. *Immunity* 2014;41:283–295.
53. Maizels RM, Withers DR. MHC-II: a mutual support system for ILCs and T cells? *Immunity* 2014;41:174–176.
54. Walker AN, Garner RE, Horst MN. Immunocytochemical detection of chitin in *Pneumocystis carinii*. *Infect Immun* 1990;58: 412–415.
55. Lee CG, Da Silva CA, Lee JY, Hartl D, Elias JA. Chitin regulation of immune responses: an old molecule with new roles. *Curr Opin Immunol* 2008;20:684–689.
56. Gingo MR, Wenzel SE, Steele C, Kessinger CJ, Lucht L, Lawther T, Busch M, Hillenbrand ME, Weinman R, Slivka WA, *et al*. Asthma diagnosis and airway bronchodilator response in HIV-infected patients. *J Allergy Clin Immunol* 2012; 129:708–714.e8.
57. Drummond MB, Huang L, Diaz PT, Kirk GD, Kleerup EC, Morris A, Rom W, Weiden MD, Zhao E, Thompson B, *et al*. Factors associated with abnormal spirometry among HIV-infected individuals. *AIDS* 2015;29: 1691–1700.
58. Chung KF, Wenzel SE, Brozek JL, Bush A, Castro M, Sterk PJ, Adcock IM, Bateman ED, Bel EH, Bleecker ER, *et al*. International ERS/ATS guidelines on definition, evaluation and treatment of severe asthma. *Eur Respir J* 2014;43:343–373.

A novel CD4$^+$ T-cell dependent murine model of *Pneumocystis* driven asthma-like pathology

Taylor Eddens[1,2], Brian T. Campfield[1,3], Katelin Serody[1], Michelle L. Manni[5], William Horne[1], Waleed Elsegeiny[1,2], Kevin J. McHugh[5], Derek Pociask[4], Kong Chen[1], Mingquan Zheng[1], John F. Alcorn[5], Sally Wenzel[6], and Jay K. Kolls[1]

[1]-Richard King Mellon Foundation Institute for Pediatric Research, Children's Hospital of Pittsburgh of UPMC, Pittsburgh, Pennsylvania, USA. [2]-University of Pittsburgh School of Medicine, Department of Immunology, Pittsburgh, Pennsylvania, USA. [3]-Division of Pediatric Infectious Diseases, Department of Pediatrics, University of Pittsburgh School of Medicine, Pittsburgh, Pennsylvania, USA. [4]-Department of Pulmonary Diseases, Critical Care, and Environmental Medicine, Tulane University School of Medicine, New Orleans, Louisiana, USA. [5]-Department of Pediatrics, Children's Hospital of Pittsburgh of UPMC, Pittsburgh, Pennsylvania, USA. [6]-Department of Pulmonary, Allergy, and Critical Care Medicine, Pittsburgh, Pennsylvania, USA.

Online Data Supplement

Methods

RNA sequencing pathway analysis

The FASTQ files from our previous study were uploaded to Illumina BaseSpace cloud-based software, aligned using TopHat version 1.0.0 and assembled with Cufflinks Assembly and DE, Version 1.1.0. Pathway analysis was then performed using iPathwayGuide, Version 1.4.0. KEGG and Disease pathways were analyzed for significance using a false discovery rate.

Purification of $CD4^+$ T-cells and adoptive transfer

Spleens from C57BL/6 mice were harvested, physically digested, and passed through a 70-µm filter. $CD4^+$ T-cells were isolated using a Stemcell™ EasySep™ Mouse kit (19852) and were subsequently enumerated. Each *Rag1*-/- mouse received 5 x 10^5 cells in 200 µL via intravenous injection. Mice were infected on the day of transfer as described above and sacrificed 6 weeks post infection.

ELISAs

96-well plates were coated overnight in a 9.2 pH carbonate buffer with 150 ng/well of *Pneumocystis* antigen, *Aspergillus fumigatus* antigen (GM3A01, Greer®), house dust mite extract (XPB70D3A2.5, Greer®), or a heat-killed *Streptococcus pneumonia* preparation. Plates were washed 5x with PBST and blocked in PBST with 5% milk for 2 hours at room temperature. Serum was diluted 1:64 (IgG assays) or 1:10 (IgE assays) in PBST with 5% milk and 100 µL was added to each well and the plate was incubated overnight at room temperature. Plates were then washed 5x with PBST and treated with

1:1000 goat anti-mouse IgG-HRP or 1:1000 goat anti-moues IgE-HRP (1030-05, Southern Biotech) diluted in blocking buffer. Following a one-hour incubation at room temperature, plates were washed 5x with PBST, developed with 1x TMB solution (BD OptEIA™, 555214), stopped with H_2SO_4 and read at 450nm. For human serum assays, bovine serum albumin was used in place of milk and rabbit anti-human IgG (A8792, Sigma®) and goat anti-human IgE (A18793, Life Technologies) were used as secondary antibodies.

Anti-PCAg Western blotting

PCAg (5 µg) or murine lung homogenate (10 µg) was denatured at 65° in LDS buffer with β-mercaptoethanol for 10 minutes and then added to a 4-20% tris-bis gel (Bio-rad) and run at 200V for 35 minutes. Following transfer to a nitrocellulose membrane (Bio-rad), the membrane was washed for 5 minutes in TBST and blocked at room temperature in TBST with 5% BSA for 2 hours. Serum samples were diluted 1:100 in TBST with 5% BSA, applied to the membrane, and incubated at 4° overnight. Membranes were washed three times with TBST for 5 minutes each, followed by addition of secondary antibody (described in ELISA) for one hour at room temperature. Membranes were then washed, developed using SuperSignal® West Pico Chemiluminescent Substrate (#34080, Thermo Scientific) and luminescence was measured for 1 second.

Flow cytometry

Whole lung cells were isolated prepared as described in the *ex vivo* whole lung cell stimulation methods. Briefly, cells were plated, centrifuged, and resuspended in surface antibodies diluted in PBS. Following a 1 hour incubation at 4°C, cells were washed and resuspended in the streptavidinBV421 (diluted 1:200). Following a 30 minute incubation at 4°C, cells were washed and fixed and permeabilized using the eBioscience FoxP3 staining kit per manufacturer's instructions. Intracellular antibodies, anti-CD45.2, and anti-CD90.2 antibodies were added and incubated at 4°C for 1 hour. Cells were then washed, resuspended, and analyzed on a BD LSR II Flow Cytometer with compensation via OneComp eBeads (eBioscience). Data analysis was conducted using FlowJo software (Treestar).

Antibodies used in these panels were diluted 1:200 in PBS unless otherwise specified and include: GATA3-FITC, diluted 1:5 (BD Pharmingen, Clone: L50-823), TCRβ-PerCP-Cy5.5 (eBioscience, Clone: H57-597), TCRγδ-PE (eBioscience, Clone: GL3), CD90.2-PE-Cy7, diluted 1:1500 (eBioscience, Clone: 53-2.1), RORγT-APC (BD Pharmingen, Clone: Q31-378), CD45.2-APC-e780 (eBioscience, Clone: 104), Streptavidin-BV421 (BioLegend, Cat: 405226), CD11b-Biotin (eBioscience, Clone: M1/70), F4/80-biotin (eBioscience, Clone: BM8), NK1.1-biotin (BD Pharmingen, Clone: PK136), CD11c-biotin (BD Pharmingen, Clone: HL3), CD19-biotin (BD Pharmingen, Clone: 1D3), TER119-biotin (BD Pharmingen, Cat: 553672). APC panel: GR-1-e450 (BD Biosciences, Clone: RB6-8C5), CD11b-APC (Biolegend, Clone: M1/70), F4/80-APC-e780 (eBioscience, Clone: BM8), SiglecF-PE (BD Biosciences, E50-2440), CD11c-FITC (eBioscience, Clone: N418).

Lung Mechanics and Airway Hyperresponsiveness Measurements

Pulmonary function was assessed during mechanical ventilation of anesthetized (90 mg/kg pentobarbital i.p.) and tracheotomized mice using a computer-controlled small-animal mechanical ventilator (FlexiVent; SCIREQ, Montreal, Quebec, Canada). Briefly, mice were mechanically ventilated at 200 breaths/min with a tidal volume of 0.25mL and a positive end expiratory pressure of 3 cmH_2O (mimicking spontaneous ventilation). The quasi-static mechanical properties of the lung (compliance and hysteresis) were calculated using pressure-volume curves derived from a step-wise inflation of the lung to a maximum pressure of 30cmH_2O. Newtonian resistance (Rn), tissue damping (G), and tissue elastance (H) were assessed prior to and following airway challenge with increasing doses of aerosolized methacholine (0, 0.75, 3.125, 12.5, and 50 mg/mL) using the forced oscillation technique and constant phase model as previously described. Multiple linear regression was used to fit measured pressure and volume in each individual mouse to the model of linear motion of the lung. Model fits that resulted in a coefficient of determination less than 0.8 were excluded.

Online Supplement Figure Legends

Supplementary Figure 1. Pathway analysis on RNA sequencing shows upregulation of pathways associated with type II immunity. A.) KEGG pathways significantly upregulated in wild type mice compared to $CD4^+$ T-cell depleted mice. B.) Individual gene expression associated with each KEGG pathway expressed as log(Fold change). C.) Disease pathways significantly upregulated in wild type mice compared to $CD4^+$ T-cell depleted mice. D.) Individual gene expression associated with each disease pathway log(Fold change).

Supplementary Figure 2. $CD4^+$ T-cells are sufficient to induce type II mediated pathology. A.) *Rag1* -/- mice received PBS (no transfer, *n*=4) or 5 x 10^5 purified $CD4^+$ T-cells (*n=4)* via intravenous injection and were infected with *Pneumocystis murina*. Six weeks post-infection, *Rag1* -/- receiving $CD4^+$ T-cells had increased gene expression of type II related genes in lung homogenate (*$p<0.05$, **$p<0.01$, student's t-test).

Supplementary Figure 3. **PCAg treated mice have increased Th2 cells and eosinophil recruitment in the lung.** A.) Following PCAg treatment, lung cells were isolated from lungs of PCAg treated or naïve mice and stimulated with PCAg or CD3/CD28 beads for 72 hours and analyzed for expression of *Gata3* and *Rorc* (** $p<0.01$). B.) Flow cytometry on $CD4^+$ T-cells demonstrates an increase in intracellular GATA3, but not RORγT, following PCAg treatment. C.) Quantification of Th2 $GATA3^+$ cells and Th17 $ROR\gamma T^+$ cells in naïve and PCAg treated mice ($p<0.05$, student's t-test). D.) qRT-PCR on *ex vivo* stimulated lung cells shows increases in *Il4* and *Il13* in

response to PCAg and a log increase in expression of *Il4*, *Il5*, and *Il13* following CD3/CD28 stimulation (*p<0.05). E.) Flow cytometry on whole lung cells shows an increase in eosinophils (SiglecF$^+$CD11b$^+$) following PCAg treatment. F.) Flow cytometry on whole lung cells shows minimal recruitment of neutrophils (CD11b$^+$Gr1$^+$) following PCAg treatment. G.) Quantification of eosinophils and neutrophils by flow cytometry shows significant increase in eosinophils following PCAg treatment (p<0.01, student's t-test).

Supplementary Figure 4. **PCAg and HDM induce similar type II responses in BALB/c mice**. A.) BALB/c mice were treated with either PCAg or HDM and type II response in whole lung was analyzed by qRT-PCR (*n*=6 per group). HDM and PCAg induce comparable type II responses in BALB/c mice (* p<0.05, ** p<0.01, one-way ANOVA with Tukey's multiple comparisons).

Supplementary Figure 5. **ST2-antibody treatment partially abrogates the pathologic Th2 response to PCAg**. C57BL/6 mice were untreated (naïve), treated with PCAg, or treated with PCAg and anti-ST2 blocking antibody (*n*=6-7). A.) Flow cytometry gating strategy for isolating ILC2 cells from whole lung. Cells were gated on lineage negative, γδ-TCR negative, CD90 high, TCRβ negative, GATA3 high (*n*=4). B.) Quantification of ILC2 cells (TCRβ$^-$GATA3$^+$) and Th2 cells (TCRβ$^+$GATA3$^+$). C.) Anti-*Pneumocystis* antigen IgG and IgE responses are unchanged with anti-ST2 treatment. D.) qRT-PCR for type II immune response genes showing decrease in type II cytokine production in anti-ST2 treated mice, but no change in mucus associated genes. E.) PAS

staining demonstrating mucus production in PCAg and PCAg mice treated with anti-ST2. (* $p<0.05$, ** $p<0.01$, *** $p<0.001$, **** $p<0.0001$, one-way ANOVA with Tukey's multiple comparisons).

Supplementary Figure 6. Individual antibody titer curves for healthy control and severe asthma patients against *Pneumocystis* and *S. pneumoniae*. A.) Individual curves for HC and SA patients showing a shift to the right in a subset of patients with SA against PCAg. B.) Individual curves for HC and SA patients showing similar antibody responses against *S. pneumoniae* (SP) antigen preparation.

Supplementary Figure 7. **Serum from a healthy control and severe asthma patient demonstrate limited reactivity to mouse lung protein**. A.) Serum samples from a healthy control and a patient with severe asthma were probed for reactivity against lung homogenate from naïve mice (N) or mice treated previously treated with PCAg (D14). Unlike the PCAg western, the same human serum samples displayed a limited reactivity to mouse protein.

Supplementary Figure 8. **Allergic sensitization in healthy control and severe asthma patients**. A.) Serum IgE shows elevation in SA patients compared to healthy controls, but no difference based on anti-PC IgG status. B.) Allergen skin testing analysis for HC, PC IgG low, and PC IgG high patients.

Supplementary Figure 9. **Peripheral blood and bronchoalveolar lavage cell analysis in healthy control and severe asthma patients**. A.) Number of neutrophils, lymphocytes, and eosinophils in peripheral blood in HC, PC IgG low, and PC IgG high patients (* $p<0.05$, ** $p<0.01$, one-way ANOVA with multiple comparisons). B.) Percentage of neutrophils, lymphocytes, eosinophils, and macrophages in the bronchoalveolar lavage of HC, PC IgG low, and PC IgG high patients.

Supplemental Figure 1

A

KEGG Pathway	p-value
Cytokine-cytokine receptor interaction	6.67×10^{-7}
Antigen processing and presentation	8.95×10^{-4}
Asthma	6.00×10^{-3}

B

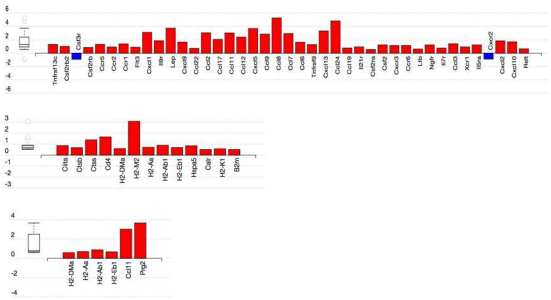

C

Disease Pathway	p-value
Allergic Rhinits	2.97×10^{-7}
Eosinophilic esophagitis	0.002
Asthma	0.029

D

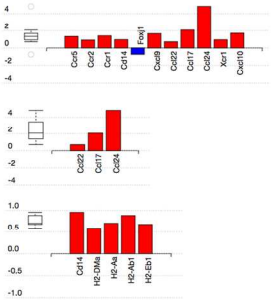

Pathway analysis on RNA sequencing shows upregulation of pathways associated with type II immunity.
177x127mm (300 x 300 DPI)

Supplemental Figure 2

A

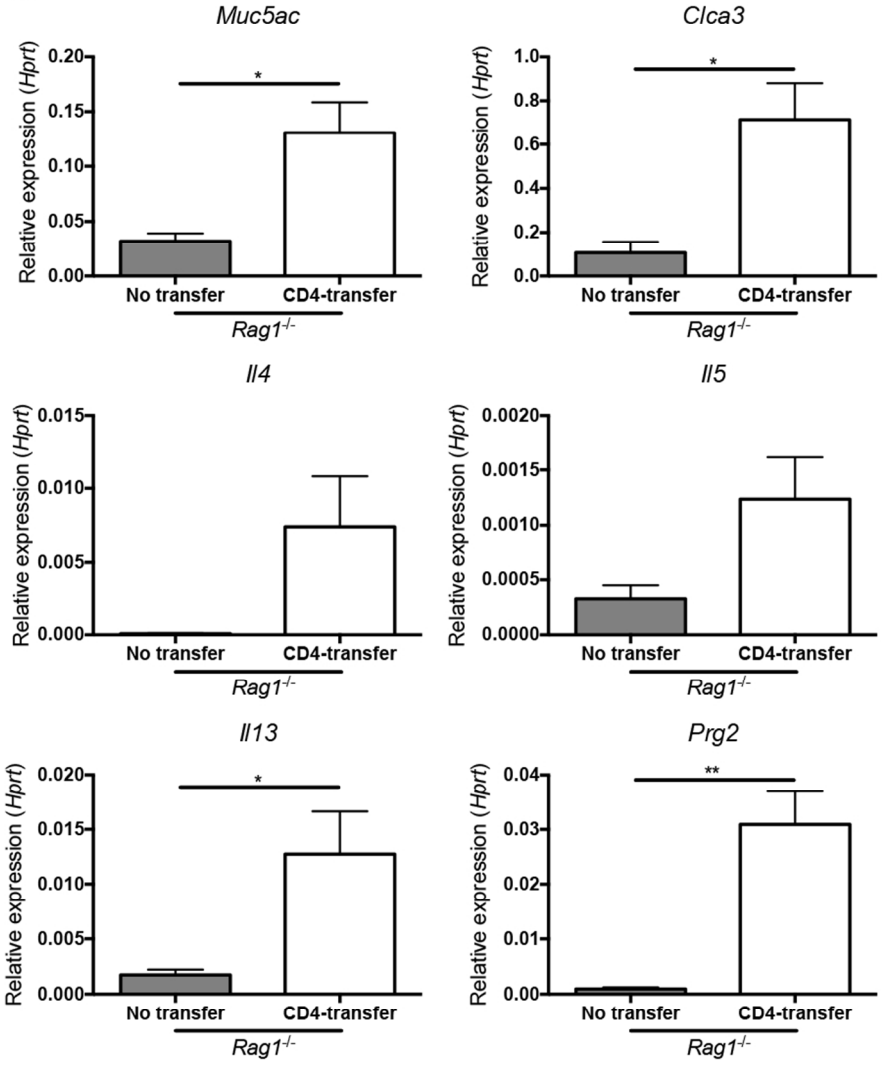

CD4+ T-cells are sufficient to induce type II mediated pathology.
82x103mm (300 x 300 DPI)

Supplemental Figure 3

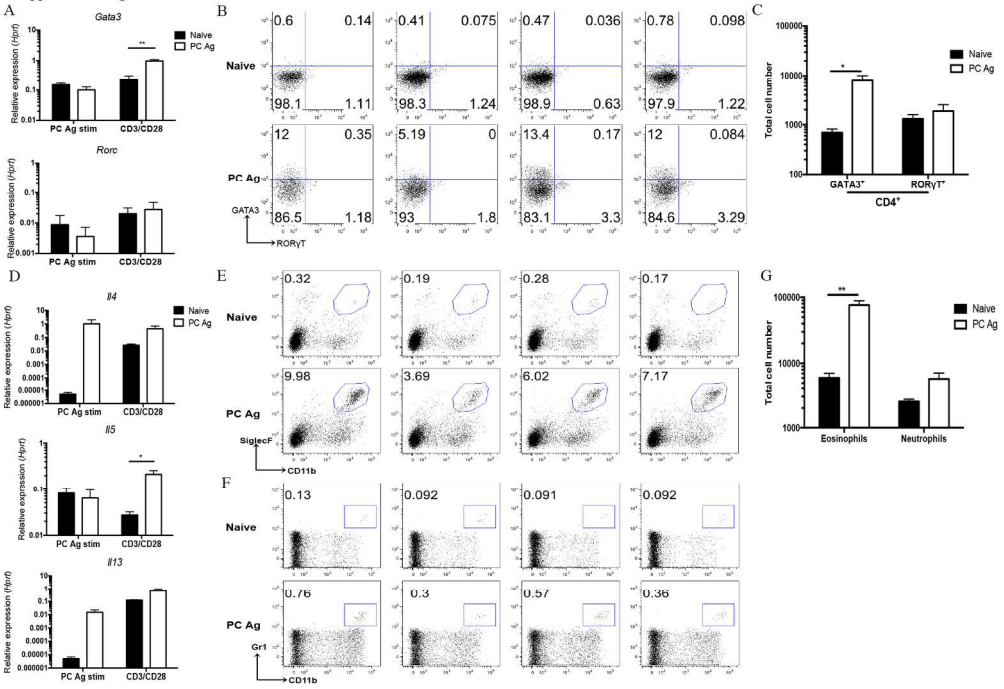

PCAg treated mice have increased Th2 cells and eosinophil recruitment in the lung.
177x127mm (300 x 300 DPI)

Supplemental Figure 4

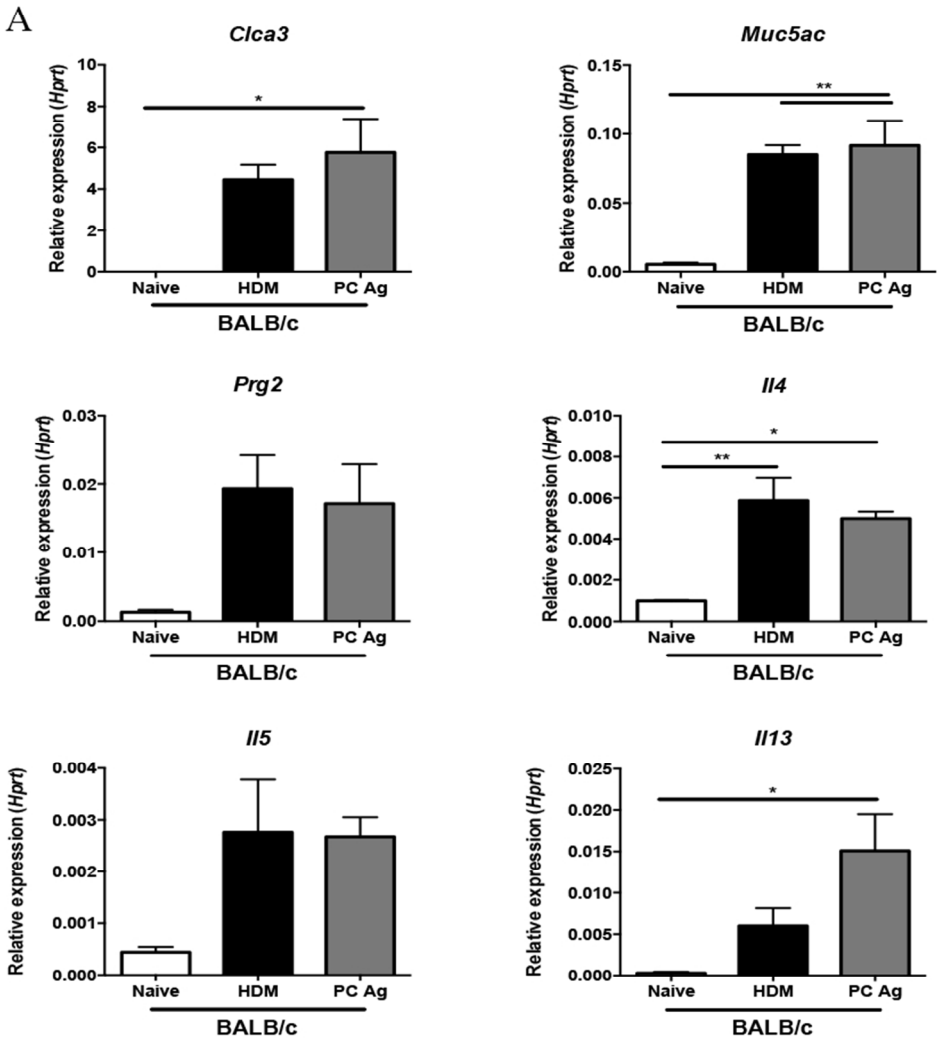

PCAg and HDM induce similar type II responses in BALB/c mice.
74x87mm (300 x 300 DPI)

Supplemental Figure 5

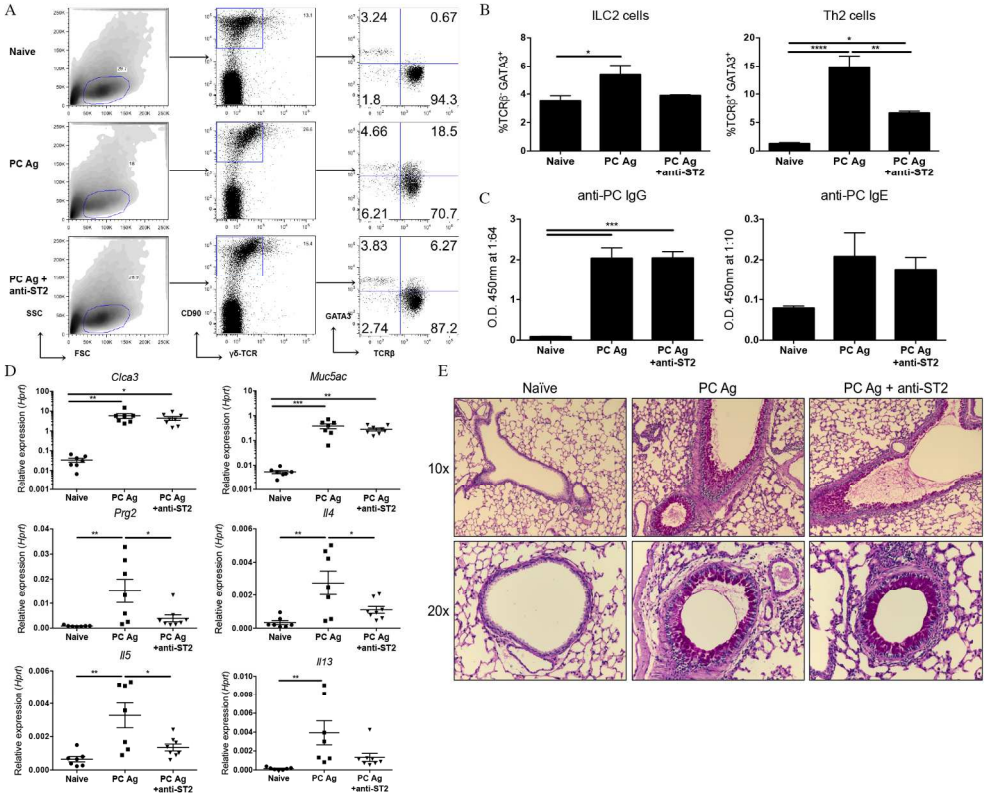

ST2-antibody treatment partially abrogates the pathologic Th2 response to PCAg
173x145mm (300 x 300 DPI)

Supplemental Figure 6

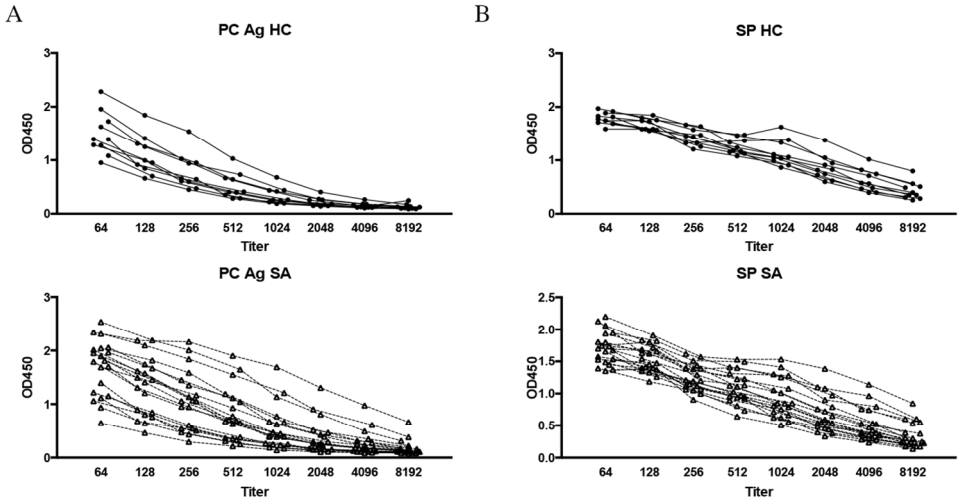

Individual antibody titer curves for healthy control and severe asthma patients against Pneumocystis and S. pneumoniae.
115x65mm (300 x 300 DPI)

Supplemental Figure 7

A

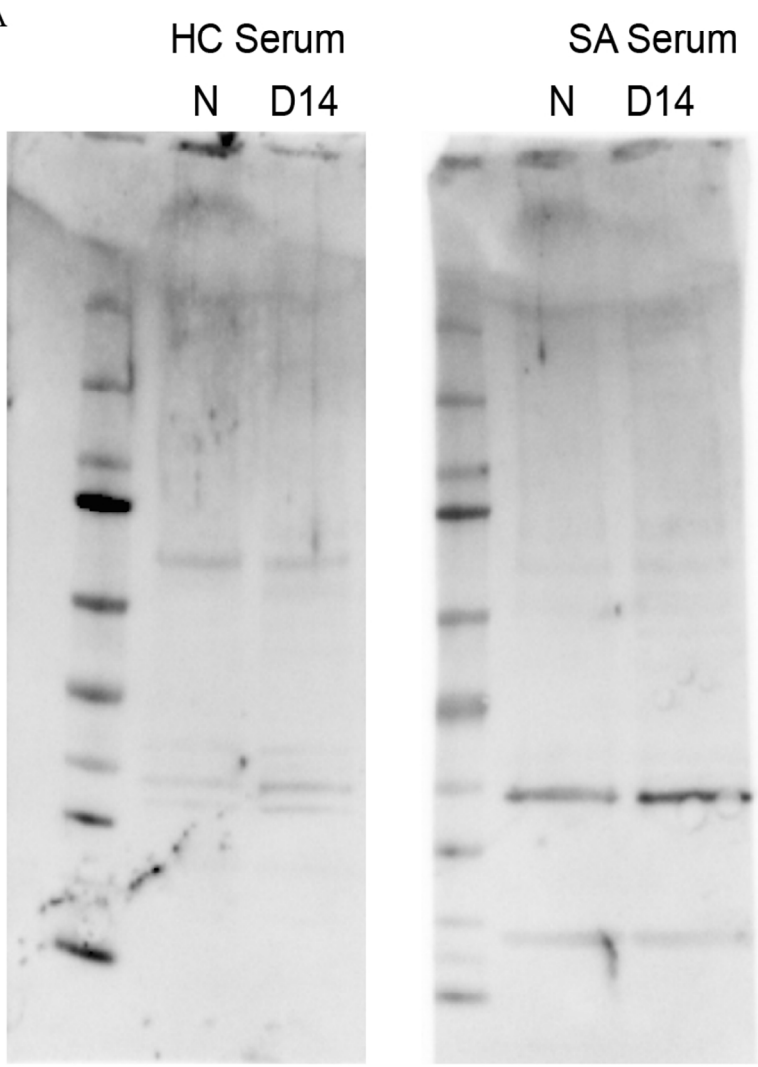

Serum from a healthy control and severe asthma patient demonstrate limited reactivity to mouse lung protein.
75x104mm (300 x 300 DPI)

Supplemental Figure 8

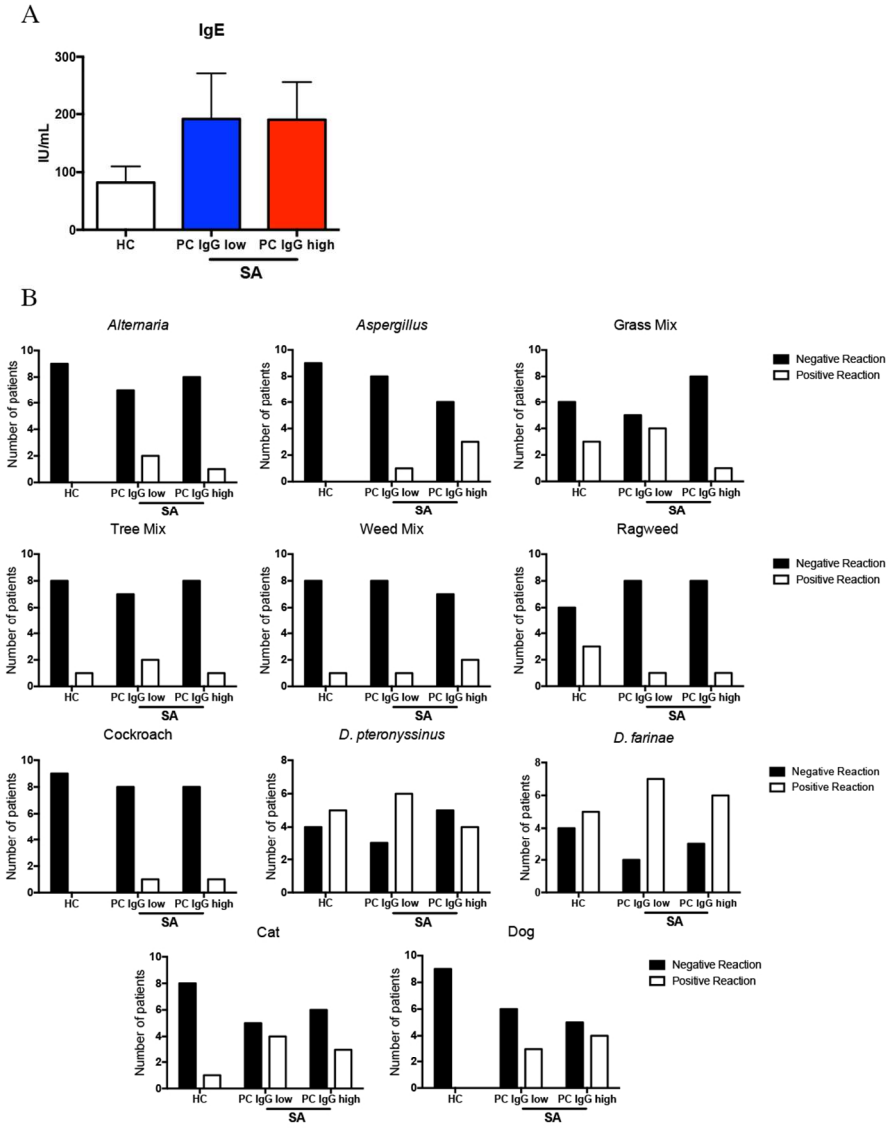

Allergic sensitization in healthy control and severe asthma patients.
95x127mm (300 x 300 DPI)

Supplemental Figure 9

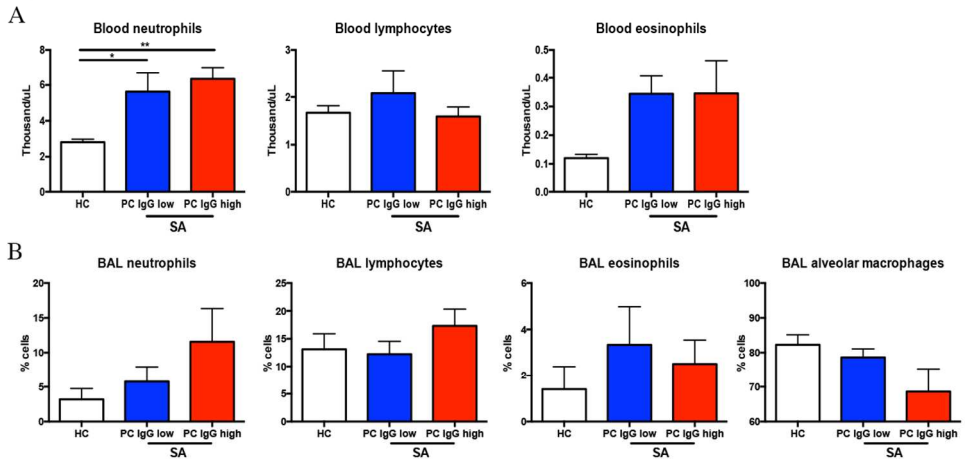

Peripheral blood and bronchoalveolar lavage cell analysis in healthy control and severe asthma patients.
115x58mm (300 x 300 DPI)

Reproduced with permission of the copyright owner. Further reproduction prohibited without permission.